**INVESTIGATION OF THE BIOFIDELITY OF HUMAN BODY MODELS AND ATD MODELS IN SLED TEST CONDITIONS**

**Autonomous Vehicle Occupant Safety Consortium**

AVOS

Paper Number 23-0288

## ABSTRACT

Unique cabin configurations associated with Automated Driving System (ADS) equipped vehicles offer seating options, such as recline, not previously available in conventional vehicles. Occupants seated in a reclined posture may be at an increased risk of submarining. There is relatively little known about the effectiveness of current restraint systems to protect reclined occupants as these systems are traditionally optimized for only upright seated postures. Anthropomorphic Testing Devices (ATDs) with the ability to differentiate between submarining and non-submarining events are vital for the development of restraint systems capable of protecting reclined occupants. This study evaluates the biofidelity of the GHBMC, THUMS, THOR, and THOR-AV finite element (FE) occupant models against two post-mortem human subject (PMHS) test series in respect of submarining behavior. The first test series evaluated upright occupant kinematics in two seat configurations defined in Uriot et al. 2015: a front-seat configuration expected to prevent submarining and a rear-seat configuration expected to allow for submarining. The second tests series evaluated upright and reclined occupant kinematics in a seat configuration as defined in UMTRI test conditions: both configurations expected to prevent submarining. Special consideration was given to pelvis kinematics and submarining response. The four FE occupant models properly differentiated between non-submarining and submarining responses in each of the evaluated test conditions. The NHTSA Biofidelity Ranking System (BRS) was used to objectively evaluate the biofidelity of the models with respect to overall occupant kinematics, as well as interaction with the restraint system (seat, anti-sub ramp, and belts). The BioRank score classifies biofidelity as *excellent*, *good*, *marginal*, or *poor*. In the first test series, the BRS scores for the interaction between all FE occupants and the restraint system corresponded to *good* biofidelity, except for THOR in the rear-seat submarining configuration (*marginal* biofidelity). In the second test series, the BRS scores for the interaction between the FE occupants and the restraint system corresponded to *marginal* biofidelity. With respect to kinematics, the BRS scores for the FE occupants ranged from *good* to *excellent* biofidelity in both test series. For each FE occupant, an average BRS score was calculated from the four test conditions. In terms of the interaction between the occupant and the restraint system, the average BRS scores for the GHBMC, THUMS, and THOR-AV corresponded to *good* biofidelity, while the average BRS score for the THOR corresponded to *marginal* biofidelity. With respect to kinematics, the GHBMC, THUMS, THOR, and THOR-AV FE models demonstrated good biofidelity.

## INTRODUCTION

ADS-equipped vehicles offer seating options for occupants not previously available in conventional vehicles, including traditional upright or recline, forward or rearward facing, or a combination of these seated postures. Occupants seated in a reclined posture may be at an increased risk of submarining as the restraint system may not have been designed with this posture considered. There is relatively little known about the effectiveness of current restraint systems to protect the reclined occupants as these systems are traditionally optimized for only upright seated postures. ATDs with the ability to differentiate between submarining and non-submarining events are vital for the development of restraint systems capable of protecting reclined occupants.

Occupant submarining has been studied over the past few decades [1]-[8]. Submarining can be defined as lap belt disengagement with the human pelvis due to slipping of the lap belt over the anterior superior iliac spine (ASIS). Submarining increases the risk of abdominal injuries due to direct loading of the lap belt to the abdomen and increases the risk of lower extremity injuries due to increased forward pelvic excursion resulting in impact of the knee with the bolster or frontal panel. Leung et al. [1] compared the Hybrid II dummy pelvis geometry with anthropometry data from pelvis bone X-rays of 28 volunteers. It was found that the Hybrid II dummy has a greater tendency to submarine than a human subject (80% for the dummy vs. 40% for the cadaver in similar tests). Leung et al. noted that the direction

and the length of sartorius were critical parameters that influenced the submarining responses of the dummy. The "sartorius" refers to the line between the ASIS and the notch between the ASIS and anterior inferior iliac spine (AIIS). The authors suggested a revision to the Hybrid II dummy pelvic bone to represent the sartorius to improve its submarining response.

Uriot et al. [2] conducted sled tests to compare the interaction between the pelvis and the lap belt for both dummies and post-mortem human subjects (PMHSs). The test setup was designed to mimic the conditions in a frontal car crash environment. The study found that the belt angle relative to the pelvis was greater for the pelvis of dummies evaluated than for those of PMHS. In 2015, Uriot et al. [3] investigated the pelvis behavior and submarining with a semi-rigid seat in sled test conditions. The semi-rigid seat had springs built in the seat pan and the anti-submarining plate. The spring stiffness for both the seat pan and anti-submarining plate can be adjusted to mimic the front- and rear-seat stiffness of a small size passenger vehicle. The PMHS did not submarine in the front-seat configuration and did not experience pelvis fractures, while the PMHS did submarine in the rear-seat configuration and did experience pelvic fractures.

Richardson et al. [4][5] studied the kinematics of the 50th percentile male PMHS in a reclined seat configuration with a nominal recline angle of 50°. The restraint system included double lap belt pre-tensioners, a shoulder belt pretensioner, a 3.5 kN shoulder belt load limiter, and a crash locking tongue. The study focused on kinematics of the pelvis, spine, and head. Four of the five PMHSs did not submarine, while one of the PMHSs experienced submarining on the inboard side. In two of the tests, the PMHSs experienced iliac wing fractures near the ASIS area where the PMHS interacted with the lap belt.

In 2019, Gepner et al. [6] compared the responses of the Global Human Body Model Consortium simplified model (GHBMC-S v1.8.4) and detailed models (GHBMC-D v4.5), and the Total Human Model for Safety (THUMS v5) in a reclined setup which served as the basis for the Richardson et al. PMHS tests [4][5]. All of these HBMs showed good pelvis engagement with the lap belt, however the GHBMC-D still submarined. In addition, large differences were observed in the pelvis and lumbar spine responses between the GHBMC and THUMS models. At the time, no PMHS test data were available to make any comparison or judge which model represents the human occupant better.

Mroz et al. [7] evaluated the effects of seat and seat belt characteristics on lumbar spine and pelvis loading with the SAFER Human Body Model (HBM) in reclined postures. The SAFER HBM responses were compared with PMHS responses using the same test condition. The HBM head, T1, T8, T11, L1, L3, and pelvis excursion, pelvis rotation, and belt forces correlated well with the PMHS results. Östh et al. [8] investigated the feasibility of restoring the occupant from reclined posture to upright during the pre-crash event with SAFER HBM. The transition could be achieved by the inertia of the occupant during pre-braking, as well as by moving the seatback. However, the occupant submarined as the pelvis did not fully return to the upright posture due to the flexibility of the lumbar spine.

Wang et al. evaluated THOR-AV in front-seat and rear-seat configurations as defined in Uriot et al. [3][10] and the upright and reclined seat configurations as defined by the University of Michigan Transportation Research Institute (UMTRI) Automated Vehicle Occupant Kinematics (AVOK) project against the corresponding PMHS test results [11]. The THOR-AV dummy kinematics demonstrated *good* to *excellent* biofidelity according to National Highway Traffic Safety Administration's (NHTSA) biofidelity ranking method (BioRank).

## OBJECTIVE

The objective of this study is to investigate the biofidelity of existing finite element (FE) occupant models in both upright and recline seated postures, considering the pelvis kinematics and submarining responses.

## METHODS

In this study, the GHBMC detailed model (v5.1), THUMS (v6.1), THOR FE model (v1.8.1), and THOR-AV FE model (v0.6) were evaluated against two PMHS tests series, in a total of four configurations. The first test series, based on Uriot et al. [2], consisted of an upright configuration representative of a front-seat in which submarining was not likely to occur, and an upright configuration representative of a rear-seat in which submarining was likely to occur. The

second test series, based on UMTRI report [9], consisted of an upright and reclined configuration which used the same front-seat setup from Uriot et al. [2]. The matrix of the simulations with additional details is shown in Table 1.

For the readers' convenience, the THOR-AV physical test data and BioRank scores from Wang et al. [10][11] were included in the tables and plots for comparison. The THOR-AV physical tests conducted in Case #1 and #2 configurations used a prototype pelvis flesh, which placed its hip joints approximately 20 mm higher than an average male. The THOR-AV physical tests conducted in Case #3 and #4 used a revised pelvis flesh with hip joint height matching that of an average male.

**Table 1**
**Simulation matrix and associated test configurations**

| Case # | Description | Test Configurations | Reference |
|---|---|---|---|
| 1 | Front-seat (22° seatback) | 50 km/h, inboard and outboard lap belt load limit 5 kN, shoulder belt load limit 7 kN | Uriot et al. [2] |
| 2 | Rear-seat (22° seatback) | 50 km/h, inboard and outboard lap belt load limit 5 kN, shoulder belt load limit 7 kN | Uriot et al. [2] |
| 3 | UMTRI (25° seatback) | 32 km/h, shoulder pretensioner only, shoulder belt load limit 3.5 kN, dynamic locking tongue | Wang et al. [11] |
| 4 | UMTRI (45° seatback) | 32 km/h, shoulder pretensioner only, shoulder belt load limit 3.5 kN, dynamic locking tongue | Wang et al. [11] |

**FE models**

The FE models of the semi-rigid seat and the restraint system were provided by LAB France for Case #1 and #2. The FE models of the semi-rigid seat and restraint system were provided by UMTRI for Case #3 and #4. The GHBMC M50-O (v5.1) and THUMS M50 (v6.1) were obtained through the respective license agreement with the model suppliers by the members of the AVOS consortium. The THOR (v1.8.1) and THOR-AV (v0.6) FE models were provided by Humanetics Innovative Solutions (Humanetics). A revised THOR-AV pelvis flesh design that allows proper buttock flesh compression to match a human was incorporated in the THOR-AV FE model v0.6 used the current study. THUMS, THOR, and THOR-AV simulations were all run on LS-Dyna vR9.3.0., and the GHBMC was run on LS-Dyna v9.3.1. The friction coefficient between occupant models and the seat and between the occupant models and the belts was 0.3 for all simulations.

**Initial Position**

For Case #1 and #2, the HBMs were pre-positioned to best match the average PMHS landmarks reported from Uriot et al. [2]. For Case #3 and #4, the HBMs were pre-positioned to best match the PMHS landmarks reported by UMTRI [9]. The landmarks for Case #3 were taken from PMHS b13109 (25°, mass 80.3 kg, stature 170.1 cm) and the landmarks from Case #4 were taken from PMHS b12795 (45°, mass 76.1 kg, stature 174.9 cm). These two specimens best matched the average-sized male. The HBMs were initially positioned with their hip joints coincident with those of the PMHS, which produced initial penetration of the buttocks with the seat pan. The seat pan was then translated downward until the initial penetration was removed. A pre-simulation was then run with the HBM skeleton held rigid while the seat pan was translated back into its original location using a boundary prescribed motion, compressing the buttocks flesh.

For THOR-AV, measurements from the dummy positioning targets were used to guide the FE model positioning. The tilt sensor readings of the pelvis, T1, and head were used to set the pelvis, torso, and head orientation. Pre-simulation was carried out to position the dummy to the prescribed positions that matched the THOR-AV physical dummy measurements. For the THOR, a similar process was used; however gravity simulation was used instead since there was no dummy positioning data available to reference.

Oasys Primer (ARUP) was used to pre-position the HBMs and ATDs. No pre-stress was carried over from the pre-positioning simulations into the main simulations. The initial positions of the FE models in the test configurations are shown in Figure 1 through Figure 3. In the UMTRI sled tests, a foam-padded knee bolster was included in the sled

fixture as a safety measure. The knee bolster was located far enough away from the lower extremities to avoid impact in a non-submarining event, yet close enough to prevent catastrophic forward excursion of the PMHS if submarining occurred. No footrest was used in the UMTRI sled tests.

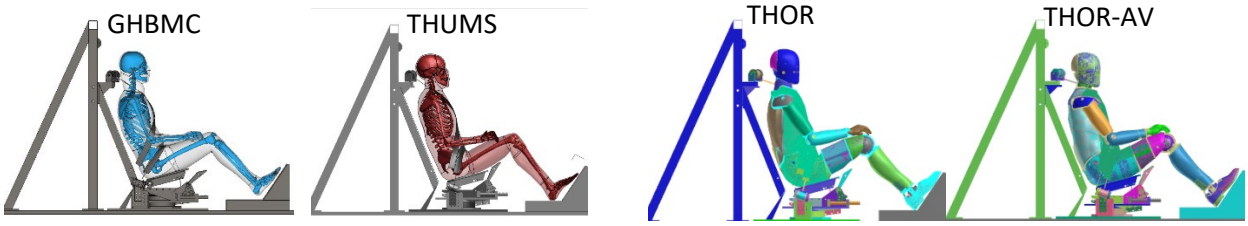


Figure 1 Initial position for the Uriot front- and rear-seat configurations.

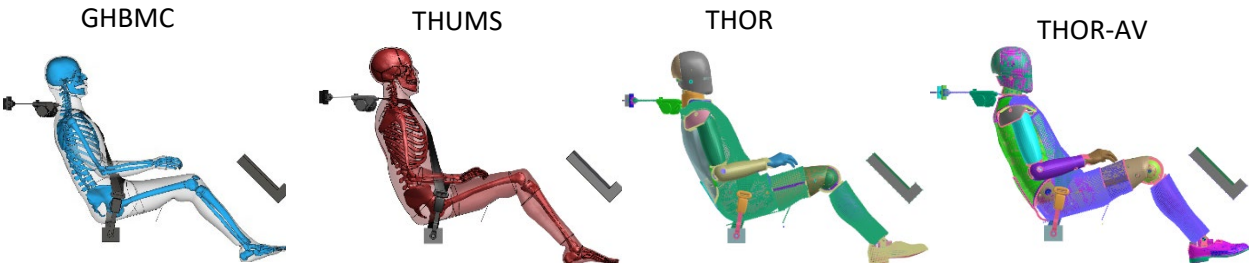


Figure 2. Initial position for the UMTRI 25° seatback configuration.

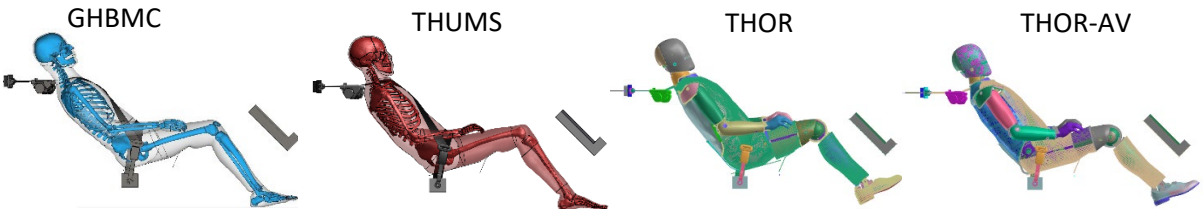


Figure 3. Initial position for the UMTRI 45° seatback configuration.

**Data Processing**

All data were filtered per SAE J211 filter class recommendations before BioRank calculation. To reduce the noise, CFC180 was applied to the accelerations of the head and the iliac bone in x-, y- and z-directions in UTMRI's PMHS data analysis (Case #3 and #4) instead of CFC1000 as recommended by SAE J211. For consistency, all four FE models used CFC180 for these data channels as well.

**BioRank Method**

The National Highway Traffic Safety Administration (NHTSA) has been developing a biofidelity ranking (BioRank) method to objectively rank the crash test dummies for its biofidelity for many years [12]-[15]. The most recent updates were documented in Kang et al. [16]. The BioRank method described in Kang et al. [16] was followed in this study. The most recent NHTSA BioRank calculation method was outlined by Rhule et al. [15]. The calculation of the BRS score is the root mean square of the Shape and Magnitude (SM) and the Phase (P) values. In 2020, NHTSA updated the method to only use the SM score [16]. The method recommends alignment of the data curves between a dummy and the PMHS corridor mean by shifting the dummy test curve until the area between the dummy data curve and the PMHS corridor mean curve is minimized. The SM score is calculated after this alignment. The shift of the dummy data curve is referred to as the Dummy Phase Shift (DPS). The DPS is monitored for each data channel. The BioRank score and the biofidelity relationship are summarized in Table 2. The typical goal for the dummy development is to achieve a BRS score equal to or less than 2.0 for each body segment and the whole dummy, which corresponds to *good* biofidelity.

**Table 2**
**Relationship between BRS scores and dummy biofidelity**

| **BRS** | **BRS ≤ 1.0** | **1.0 <BRS≤ 2.0** | **2.0 < BRS ≤ 3.0** | **BRS > 3.0** |
|---|---|---|---|---|
| Biofidelity | *Excellent* | *Good* | *Marginal* | *Poor* |

## RESULTS

The BioRank scores were calculated for each test configuration. The interaction of the FE occupant with the restraint system was evaluated separately from the occupant kinematics. The BRS scores are reported in this section and the data plots with biofidelity corridors are presented in the Appendix.

**Uriot Front Seat (Case #1)**

The BRS scores for the restraint system are summarized in Table 3. In general, most of the BRS scores for the restraint system are less than 2.0, corresponding to either *excellent* or *good* biofidelity. However, the BRS scores of the seat-pan force in the z-direction and the seat-pan y-rotation were rated as *marginal* or *poor* for all four FE occupant models with a BRS scores greater than 2.0, except the force in the z-direction for THUMS which was rated as good. The average of the restraint system BRS scores are 1.48, 1.56, 1.51, and 1.54 for the GHBMC, THUMS, THOR FE, and THOR-AV FE models, respectively; all corresponding to *good* biofidelity.

In the front-seat, upright configuration defined in Uriot et al.[2], neither the HBM nor the ATD FE occupants submarined, consistent with the PMHS response. The kinematics BRS scores for the occupant models are summarized in Table 4. There are limited parameters from the PMHS tests for biofidelity evaluation in this test configuration. Out of these parameters evaluated, the majority of them have BRS scores less than 1.0, corresponding to *excellent* biofidelity. The average BRS scores for the GHBMC, THUMS, THOR FE, and THOR-AV FE, are 0.84, 0.72, 0.61 and 0.70 respectively, all corresponding to *excellent* biofidelity.

**Table 3**
**BRS scores of the restraint system for the GHBMC, THUMS, THOR, and THOR-AV FE models in the front-seat test configuration**

| | **GHBMC** | | **THUMS** | | **THOR FE** | | **THOR-AV FE** | |
|---|---|---|---|---|---|---|---|---|
| **Restraint System** | BRS | DPS(ms) | BRS | DPS(ms) | BRS | DPS(ms) | BRS | DPS(ms) |
| Seat (average) | 1.92 | 3 | 1.90 | -1 | 1.98 | -1 | 2.01 | -1 |
| Seat Pan Force X | 1.68 | 2 | 1.36 | -1 | 1.04 | 1 | 1.30 | 3 |
| Seat Pan Force Z | 2.06 | 8 | 1.88 | -1 | 3.16 | -7 | 2.67 | -7 |
| Seat Pan Rotation Y | 3.17 | -4 | 3.18 | -4 | 2.97 | -2 | 3.19 | 0 |
| Anti-Sub Plate Rotation Y | 0.79 | 5 | 1.18 | 0 | 0.75 | 5 | 0.89 | 0 |
| Belt (average) | 1.03 | -1 | 1.23 | -2 | 1.03 | -2 | 1.06 | -1 |
| Upper Shoulder Belt Force | 1.01 | -1 | 0.58 | -3 | 0.84 | 2 | 0.86 | 1 |
| Lower Shoulder Belt Force | 1.35 | 1 | 1.39 | 1 | 1.06 | 2 | 1.23 | 0 |
| Inner Lap Belt Force | 1.48 | 1 | 1.05 | -2 | 0.84 | -4 | 0.82 | -4 |
| Outer Lap Belt Force | 0.89 | -1 | 0.61 | -1 | 0.77 | -5 | 0.72 | -4 |
| Inner Lap Belt Rotation Y | 0.90 | -8 | 1.01 | -6 | 1.68 | -9 | 2.31 | 3 |
| Outer Lap Belt Rotation Y | 1.14 | 0 | 3.01 | 0 | 1.40 | 0 | 1.07 | 0 |
| Pelvis to Lab Belt Rotation Y | 0.46 | -2 | 0.92 | -3 | 0.67 | 0 | 0.45 | -1 |
| **Overall Restraint Average** | **1.48** | **1** | **1.56** | **-2** | **1.51** | **-2** | **1.54** | **-1** |

**Table 4**
**The BRS scores of the GHBMC, THUMS, THOR, and THOR-AV models in the front-seat test configuration**

| | GHBMC | | THUMS | | THOR | | THOR-AV | |
|---|---|---|---|---|---|---|---|---|
| **Body Region** | BRS | DPS(ms) | BRS | DPS(ms) | BRS | DPS(ms) | BRS | DPS (ms) |
| Thorax | 0.85 | 1 | 0.73 | 0 | 0.63 | 4 | 0.81 | 0 |
| Chest Acceleration | 0.85 | 1 | 0.73 | 0 | 0.63 | 4 | 0.81 | 0 |
| Pelvis (average) | 0.82 | 1 | 0.70 | 3 | 0.60 | 0 | 0.60 | 0 |
| Pelvis Resultant Acceleration | 1.43 | 0 | 1.08 | 0 | 0.74 | -7 | 1.14 | -6 |
| Pelvis Rotation Y | 0.76 | 2 | 0.90 | 9 | 0.48 | 5 | 0.45 | 3 |
| Pelvis Displacement X | 0.28 | 0 | 0.12 | 1 | 0.57 | 2 | 0.22 | 2 |
| **Overall Average** | **0.84** | **1** | **0.72** | **1** | **0.61** | **2** | **0.70** | **0** |

The pelvis x-displacement and y-rotation for all four FE models were well within the PMHS corridors, as shown in Figure 4. As mentioned earlier, the THOR-AV tests in Cases #1 and #2 were from a prototype pelvis flesh that placed the dummy hip joint higher by approximately 20 mm than an average male. A revised THOR-AV pelvis flesh design that allows proper buttock flesh compression to match a human was incorporated in the THOR-AV FE model v0.6 in this study.

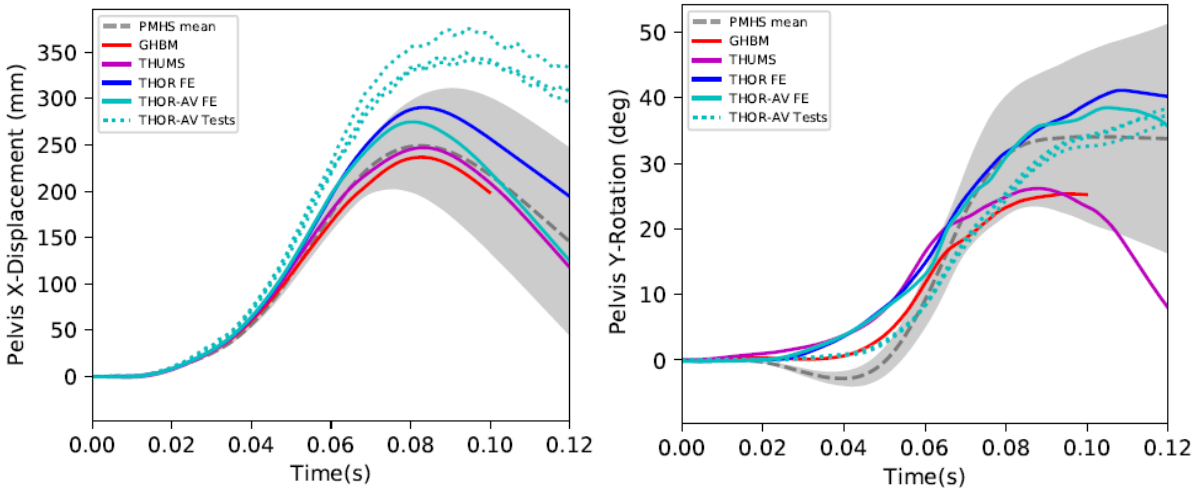


Figure 4. Pelvis x-displacement (left) and pelvis y-rotation (right) in the front-seat test configuration.

**Uriot Rear Seat (Case #2)**

The BRS scores for the restraint system are summarized Table 5. Overall, the interaction between the restraint system and the dummy is reasonable with a majority of the BRS scores less than 2.0. The BRS scores for seat-pan force in the z-direction for the GHBMC and THUMS HBMs are 2.32 and 2.28, respectively; both corresponding to *marginal* biofidelity. The BRS scores of the seat pan force in the z-direction for the THOR and THOR-AV ATDs are 4.85 and 3.12, respectively; both corresponding to *poor* biofidelity. The BRS score of the seat-pan rotation for the THOR is 4.35, corresponding to *poor* biofidelity. In addition, *marginal* or *poor* biofidelity of the lap belt rotation and the lap belt relative-to-pelvis rotation was observed for the GHBMC model. *Marginal* biofidelity of the outer lap belt force and lap belt rotation for the THOR-AV model was observed as well. Overall, the GHBMC, THUMS, THOR FE, and THOR-AV FE models have BRS scores of 1.34, 1.18, 2.03, and 1.80 for the restraint system; corresponding to *good, good, marginal,* and *good* biofidelity, respectively.

In the rear-seat, upright test configuration defined in Uriot et al. [2], all HBM and ATD models submarined, consistent with the PMHS responses. The kinematics BRS scores for the occupant models are summarized in Table 6. The average BRS scores of the four models are 0.93, 0.83, 0.71 and 0.84; all corresponding to *excellent* biofidelity.

**Table 5**

**The BRS scores of the restraint system for the GHBMC, THUMS, THOR, and THOR-AV models in the rear-seat test configuration**

| | GHBMC | | THUMS | | THOR FE | | THOR-AV FE | |
|---|---|---|---|---|---|---|---|---|
| **Restraint System** | BRS | DPS (ms) | BRS | DPS (ms) | BRS | DPS (ms) | BRS | DPS (ms) |
| Seat (average) | 1.20 | -4 | 1.33 | -6 | 3.01 | -4 | 1.88 | -2 |
| Seat Pan Force X | 0.88 | -4 | 0.83 | -5 | 1.44 | 0 | 1.46 | 0 |
| Seat Pan Force Z | 2.32 | -2 | 2.28 | -5 | 4.85 | 0 | 3.12 | 0 |
| Seat Pan Rotation Y | 1.24 | -3 | 1.49 | -6 | 4.35 | -10 | 1.74 | -7 |
| Anti-Sub Plate Rotation Y | 0.36 | -8 | 0.72 | -9 | 1.38 | -6 | 1.18 | 0 |
| Belt (average) | 1.48 | 2 | 1.02 | 0 | 1.06 | 1 | 1.72 | 1 |
| Upper Shoulder Belt Force | 0.71 | 2 | 0.80 | 1 | 0.84 | 6 | 0.82 | 3 |
| Lower Shoulder Belt Force | 0.56 | 1 | 1.25 | 0 | 0.80 | 4 | 0.80 | 1 |
| Inner Lap Belt Force | 0.54 | 7 | 0.61 | 6 | 0.80 | 0 | 1.85 | 10 |
| Outer Lap Belt Force | 0.62 | 7 | 0.44 | 5 | 0.76 | 1 | 2.07 | 8 |
| Inner Lap Belt Rotation Y | 3.58 | 0 | 2.21 | -2 | 1.66 | -8 | 2.42 | -6 |
| Outer Lap Belt Rotation Y | 2.13 | 0 | 0.83 | -9 | 1.71 | 0 | 2.60 | 0 |
| Pelvis to Lab Belt Rotation Y | 2.24 | -3 | 1.03 | -2 | 0.84 | 0 | 1.47 | -7 |
| **Overall Average** | **1.34** | **-1** | **1.18** | **-3** | **2.03** | **-2** | **1.80** | **0** |

**Table 6**

**The BRS scores for the GHBMC, THUMS, THOR, and THOR-AV models in the rear-seat test configuration**

| | GHBMC | | THUMS | | THOR FE | | THOR-AV FE | |
|---|---|---|---|---|---|---|---|---|
| **Body Region** | **BRS** | **DPS** (ms) | **BRS** | **DPS** (ms) | **BRS** | **DPS** (ms) | **BRS** | **DPS** (ms) |
| Thorax | 0.80 | 5 | 0.72 | -2 | 0.77 | -1 | 0.96 | 0 |
| Chest Acceleration | 0.80 | 5 | 0.72 | -2 | 0.77 | -1 | 0.96 | 0.4 |
| Pelvis (average) | 1.06 | 0 | 0.94 | 2 | 0.64 | 0 | 0.71 | 0 |
| Pelvis Resultant Acceleration | 1.20 | 2 | 1.05 | 7 | 0.64 | -4 | 0.98 | -3 |
| Pelvis Rotation Y | 0.95 | 4 | 0.92 | 2 | 0.61 | 6 | 0.70 | 3 |
| Pelvis Displacement X | 1.04 | -5 | 0.86 | -2 | 0.68 | -1 | 0.45 | -1 |
| **Overall Average** | **0.93** | **3** | **0.83** | **0** | **0.71** | **0** | **0.84** | **0** |

The pelvis x-displacement and y-rotation for the four FE models were well within the PMHS corridors, as shown in Figure 5.

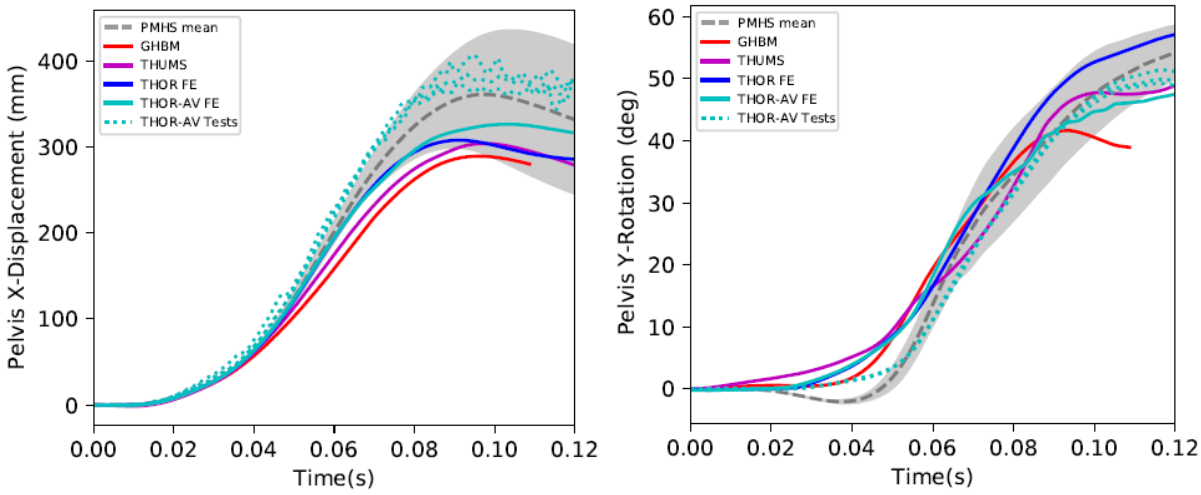


Figure 5. Pelvis x-displacement and y-rotation in the rear-seat test configuration

**UMTRI 25° (Case #3)**

The BRS scores for the restraint system are summarized in Table 7. The BRS scores of the seat force in the z-direction for the THUMS, THOR, and THOR-AV models are 2.12, 2.59 and 2.62, respectively; all corresponding to *marginal* biofidelity. The seat-pan rotation and anti-submarine plate rotation of all four models showed either *marginal* or *poor* biofidelity. The BRS scores of the lap belt forces at the outer side and the buckle locations are greater than 2.0 for THUMS, corresponding to *marginal* biofidelity. The overall restraint system response showed *marginal* biofidelity for the GHBMC, THUMS, THOR, and THOR-AV models.

In this front-seat, upright test configuration, neither the HBM nor the ATD models submarined, consistent with the PMHS responses reported by UMTRI. The kinematics BRS scores for the occupant models are summarized in Table 8. The BRS scores of all parameters evaluated are less than 2.0 with many of them less than 1.0, corresponding to either *good* or *excellent* biofidelity. The average kinematic BRS scores for the GHBMC, THUMS, THOR, and THOR-AV models are 0.94 (*excellent* biofidelity), 1.06 (*good* biofidelity), 1.26 (*good* biofidelity), and 0.87(*excellent* biofidelity), respectively.

**Table 7**

**The BRS scores of the restraint system for the GHBMC, THUMS, THOR, and THOR-AV models in the UMTRI 25° test configuration**

| | GHBMC | | THUMS | | THOR | | THOR-AV | |
|---|---|---|---|---|---|---|---|---|
| **Restraint System** | **BRS** | **DPS** (ms) | **BRS** | **DPS** (ms) | **BRS** | **DPS** (ms) | **BRS** | **DPS** (ms) |
| Seat (average) | 2.77 | 3 | 2.61 | 0 | 2.84 | 1 | 2.88 | 2 |
| Seat Force X | 1.69 | 6 | 1.49 | 1 | 1.19 | 0 | 1.19 | 6 |
| Seat Force Z | 1.82 | 6 | 2.12 | -1 | 2.59 | 5 | 2.62 | 4 |
| Seat Pan Rotation Y | 2.85 | 2 | 2.54 | -1 | 3.70 | 0 | 2.56 | 0 |
| Anti-Sub Plate Rotation Y | 4.71 | 0 | 4.29 | 0 | 3.90 | 0 | 5.17 | 0 |
| Belt (average) | 1.49 | -3 | 1.94 | -4 | 1.73 | 0 | 1.28 | -3 |
| Outer Lap Belt Force | 1.69 | 0 | 2.39 | -2 | 1.29 | -4 | 1.16 | -4 |
| Lap Belt Buckle Force | 1.58 | -2 | 2.16 | -5 | 2.01 | -1 | 1.40 | -2 |
| Upper Shoulder Belt Force | 1.20 | -5 | 1.29 | -6 | 1.90 | 6 | 1.29 | -2 |
| **Restraint Overall Average** | **2.13** | **0** | **2.28** | **-2** | **2.29** | **1** | **2.08** | **0** |

**Table 8**

**The BRS scores for the GHBMC, THUMS, THOR, and THOR-AV models in the UMTRI 25° test configuration**

| | GHBMC | | THUMS | | THOR | | THOR-AV | |
|---|---|---|---|---|---|---|---|---|
| **Body Region** | BRS | DPS (ms) | BRS | DPS (ms) | BRS | DPS (ms) | BRS | DPS (ms) |
| Head (average) | 1.07 | -1 | 1.28 | 1 | 1.03 | -1 | 0.63 | 2 |
| Head Acceleration X | 0.93 | -7 | 1.52 | 0 | 1.36 | -6 | 0.81 | -5 |
| Head Acceleration Z | 1.40 | 0 | 1.41 | 0 | 1.34 | 0 | 0.73 | 0 |
| Head Angular Velocity Y | 1.00 | 0 | 0.93 | 0 | 1.27 | 0 | 0.97 | 6 |
| Head Displacement X | 1.55 | 2 | 1.63 | 3 | 0.28 | 1 | 0.32 | 1 |
| Head Displacement Z | 0.47 | 0 | 0.92 | 0 | 0.89 | 0 | 0.33 | 9 |
| Spine (average) | 0.90 | -1 | 1.17 | 0 | 1.46 | 0 | 0.92 | -1 |
| T1 Acceleration X | 1.17 | 0 | 1.37 | -5 | 1.19 | 0 | 1.05 | -1 |
| T1 Acceleration Z | 1.09 | 0 | 1.12 | 0 | 1.68 | 0 | 1.35 | 0 |
| T1 Displacement X | 0.90 | -1 | 1.81 | 4 | 1.47 | -1 | 0.88 | 1 |
| T1 Displacement Z | 0.65 | 0 | 1.40 | 0 | 1.79 | 0 | 0.32 | 0 |
| T8 Displacement X | 0.72 | 1 | 1.41 | 3 | NA | NA | NA | NA |
| T8 Displacement Z | 0.75 | 0 | 0.59 | 0 | NA | NA | NA | NA |
| T12 Acceleration X | 1.66 | -5 | 1.40 | -3 | 1.52 | 1 | 1.23 | -3 |
| T12 Acceleration Z | 0.96 | 0 | 0.85 | -4 | 1.05 | -4 | 0.94 | -4 |
| T12 Displacement X | 0.57 | 0 | 1.13 | 2 | 1.26 | 2 | 1.17 | 2 |
| T12 Displacement Z | 0.54 | 0 | 0.29 | 0 | 1.75 | 2 | 0.43 | 0 |
| L4 Acceleration X | 1.17 | 1 | 1.81 | -1 | NA | NA | NA | NA |
| L4 Acceleration Z | 0.64 | -5 | 0.82 | 1 | NA | NA | NA | NA |
| Pelvis (average) | 0.85 | 0 | 0.74 | 1 | 1.28 | -1 | 1.06 | 0 |
| Pelvis Acceleration X | 1.41 | -4 | 1.39 | 0 | 1.81 | 0 | 1.32 | 0 |
| Pelvis Acceleration Z | 1.59 | -2 | 0.74 | -1 | 1.25 | -5 | 1.07 | -5 |
| Pelvis Angular Velocity Y | 0.96 | 0 | 0.81 | 4 | 0.99 | 2 | 0.87 | 0 |
| Pelvis Rotation Y | 0.48 | 6 | 0.82 | 0 | 0.73 | 0 | 0.36 | 0 |
| Pelvis Displacement X | 0.16 | 0 | 0.27 | 1 | 1.24 | 0 | 0.90 | 2 |
| Pelvis Displacement Z | 0.47 | 0 | 0.40 | 0 | 1.67 | 0 | 1.84 | 0 |
| **HBM/ATD Overall Average** | **0.94** | **-1** | **1.06** | **0** | **1.26** | **-1** | **0.87** | **0** |

Note: NA – no data available, the dummies were not instrumented for these channels

The head center of gravity, T1, T8, T12, and hip joint mid-sagittal trajectory overlays are illustrated in Figure 6. Due to anthropometric differences between the FE occupants and physical surrogates, the starting location of these trajectories are different. For illustrative purposes, each trajectory was transformed so that the starting location of the trajectory for a particular body region was aligned with the corresponding starting location of the THUMS FE model.

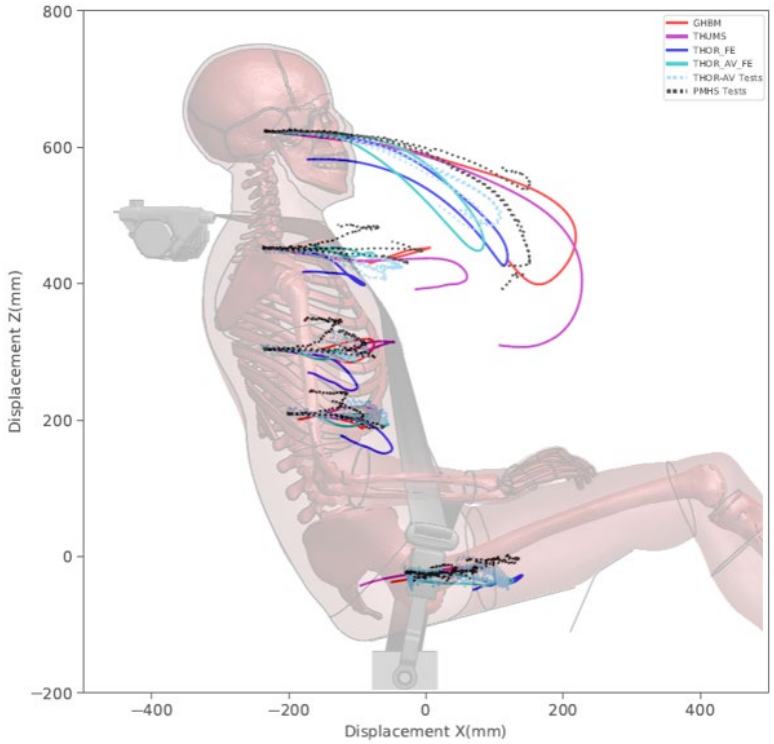


Figure 6. Trajectory overlays for the GHBMC, THUMS, THOR, THOR-AV models and the PMHS data for Case #3

**UMTRI 45° (Case #4)**

The BRS scores for the restraint system are summarized in Table 9. Many of the parameters evaluated have a BRS score less than 2.0, corresponding to *good* biofidelity. However, the anti-submarining plate rotation for all models is greater than 4.29, corresponding to *poor* biofidelity, which affected the overall biofidelity results. The seat force in the x-direction for the GHBMC model has a BRS score of 2.30, corresponding to *marginal* biofidelity, and the lap belt buckle force and the shoulder belt force for the THOR model have BRS scores of 2.69 and 2.80, respectively, both corresponding to *marginal* biofidelity. The overall biofidelity for all models is *marginal*.

**Table 9**

**The BRS scores of restraint system for the GHBMC, THUMS, THOR, and THOR-AV models in the UMTRI 45° test configuration**

| | GHBMC | | THUMS | | THOR | | THOR-AV | |
|---|---|---|---|---|---|---|---|---|
| **Restraint System** | BRS | DPS (ms) | BRS | DPS (ms) | BRS | DPS (ms) | BRS | DPS (ms) |
| Seat | 3.28 | 1 | 2.42 | -2 | 2.63 | 1 | 3.22 | 2 |
| Seat Force X | 2.30 | -1 | 1.74 | -6 | 1.59 | 1 | 1.93 | 4 |
| Seat Force Z | 1.47 | 4 | 1.75 | -5 | 1.17 | 4 | 1.40 | 4 |
| Seat Pan Rotation Y | 1.84 | 0 | 1.89 | 3 | 2.00 | 0 | 1.17 | 0 |
| Anti-Sub Plate Rotation Y | 7.52 | 0 | 4.29 | 0 | 5.78 | 0 | 8.38 | 0 |
| Belt | 1.85 | 0 | 1.62 | -3 | 2.46 | -1 | 1.41 | 1 |
| Outer Lap Belt Force | 1.69 | 0 | 1.80 | -3 | 1.88 | -2 | 1.16 | 4 |
| Lap Belt Buckle Force | 1.87 | 2 | 1.67 | -2 | 2.69 | -1 | 1.20 | 0 |
| Upper Shoulder Belt Force | 1.99 | -1 | 1.39 | -3 | 2.80 | -2 | 1.88 | 0 |
| **Restraint Overall Average** | **2.56** | **1** | **2.02** | **-2** | **2.55** | **0** | **2.32** | **2** |

In this front-seat, reclined test configuration, neither the HBM nor the ATD models submarined, consistent with the PMHS responses reported by UMTRI. The kinematics BRS scores for the occupant models are summarized in Table 10. Most of the parameters evaluated have a BRS score less than 2.0, with many of them less than 1.0 for all four models; corresponding to either a *good* or *excellent* biofidelity. The average kinematic BRS scores for the GHBMC, THUMS, THOR, and THOR-AV models are 1.28, 1.45, 1.36, 1.12, respectively; all corresponding to *good* biofidelity.

**Table 10**

**The BRS scores for the GHBMC, THUMS, THOR, and THOR-AV models in the UMTRI 45° test condition**

| | GHBM | | THUMS | | THOR | | THOR-AV | |
|---|---|---|---|---|---|---|---|---|
| **Body Regions** | BRS | DPS(ms) | BRS | DPS(ms) | BRS | DPS(ms) | BRS | DPS(ms) |
| Head | 1.51 | 1 | 2.19 | 0 | 1.29 | 0 | 0.86 | -1 |
| Head Acceleration X | 1.66 | 0 | 1.67 | 0 | 1.08 | -7 | 0.66 | -4 |
| Head Acceleration Z | 1.27 | 0 | 1.98 | 0 | 2.28 | 0 | 0.87 | 5 |
| Head Angular Velocity Y | 2.16 | 0 | 2.81 | 0 | 2.01 | 3 | 1.32 | 5 |
| Head Displacement X | 1.19 | -2 | 1.10 | -2 | 0.65 | -3 | 0.84 | -3 |
| Head Displacement Z | 1.25 | 8 | 3.39 | 0 | 0.42 | 6 | 0.59 | -7 |
| Spine | 0.96 | -1 | 1.22 | -2 | 1.61 | -2 | 1.14 | -1 |
| T1 Acceleration X | 0.66 | 0 | 0.63 | 0 | 0.63 | -6 | 0.62 | 0 |
| T1 Acceleration Z | 0.77 | 0 | 0.71 | 0 | 1.16 | 0 | 0.90 | 0 |
| T1 Displacement X | 0.76 | -4 | 2.42 | 1 | 1.43 | -4 | 3.14 | -4 |
| T1 Displacement Z | 0.91 | 0 | 1.67 | 0 | 2.23 | 0 | 0.66 | -3 |
| T8 Displacement X | 0.76 | -4 | 0.16 | -1 | NA | NA | NA | NA |
| T8 Displacement Z | 0.91 | 0 | 2.29 | 0 | NA | NA | NA | NA |
| T12 Acceleration X | 1.47 | 0 | 1.11 | -2 | 1.44 | 0 | 0.86 | -1 |
| T12 Acceleration Z | 0.69 | -3 | 0.70 | -6 | 0.88 | -9 | 0.64 | 1 |
| T12 Displacement X | 1.06 | -2 | 0.20 | -1 | 1.25 | 1 | 0.47 | -1 |
| T12 Displacement Z | 2.10 | 0 | 2.83 | 0 | 3.83 | 0 | 1.79 | 0 |
| L4 Acceleration X | 0.77 | -2 | 1.31 | -7 | NA | NA | NA | NA |
| L4 Acceleration Z | 0.70 | 5 | 0.67 | -5 | NA | NA | NA | NA |
| Pelvis | 1.37 | 1 | 0.92 | -2 | 1.18 | 1 | 1.36 | 1 |
| Pelvis Acceleration X | 2.13 | 0 | 1.42 | -9 | 2.21 | 0 | 1.68 | 0 |
| Pelvis Acceleration Z | 1.35 | -2 | 1.03 | -4 | 1.18 | 2 | 0.94 | 5 |
| Pelvis Angular Velocity Y | 1.25 | 0 | 1.34 | -5 | 0.60 | 1 | 1.41 | 0 |
| Pelvis Rotation Y | 1.13 | 7 | 0.95 | 0 | 0.10 | 1 | 1.61 | 0 |
| Pelvis Displacement X | 0.44 | 0 | 0.33 | 0 | 0.89 | 1 | 0.61 | -1 |
| Pelvis Displacement Z | 1.94 | 0 | 0.47 | 7 | 2.11 | 0 | 1.90 | 0 |
| **HBM/ATD Overall Average** | **1.28** | **0** | **1.45** | **-1** | **1.36** | **-1** | **1.12** | **0** |

The trajectory overlays are illustrated in Figure 7.

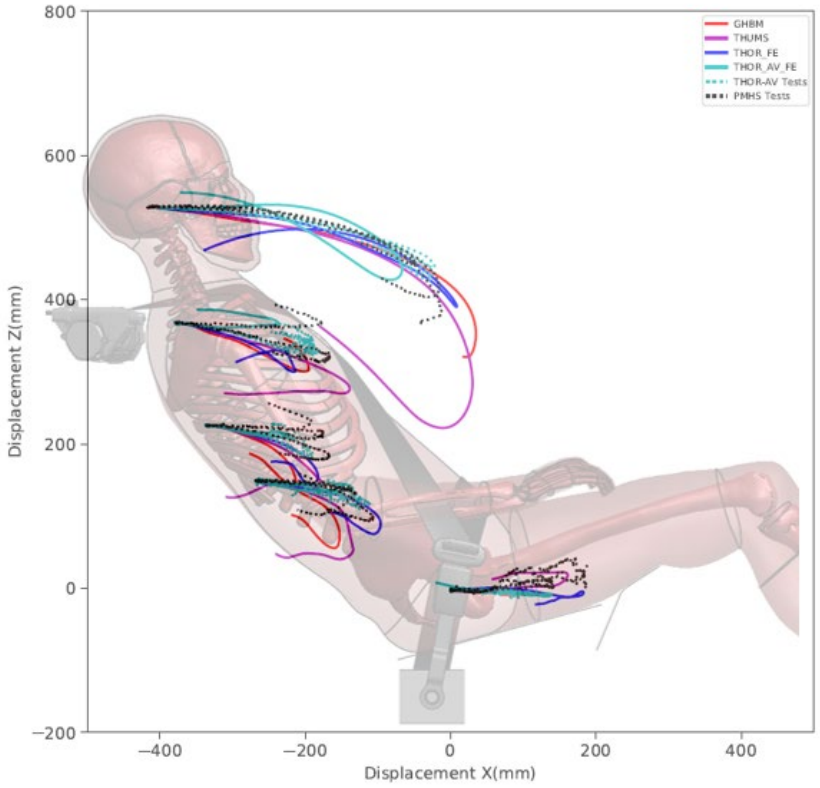


Figure 7. Trajectory overlays for the GHBMC, THUMS, THOR and THOR-AV models and the PMHS data for Case #4.

**Overall Averages (Cases #1-4)**

The overall averages of the restraint system for these four test configurations are summarized in Table 11, and the overall kinematics average of the responses of the FE occupant models for the four test configurations are summarized in Table 12. The biofidelity of the THOR-AV was evaluated by Wang et al. [10][11]. For the reader's convenience, the THOR-AV dummy's BRS scores are included for references. Except for the THOR FE model, the restraint system BRS scores are within 2.0, corresponding to *good* biofidelity. The kinematic BRS scores for the GHBMC, THUMS, THOR, and THOR-AV models are close to 1.0, corresponding to *good* or *excellent* biofidelity.

**Table 11**
**The average restraint system BRS scores for the GHBMC, THUMS, THOR, THOR-AV models and the THOR-AV test**

| | GHBMC | | THUMS | | THOR FE | | THOR-AV FE | | THOR-AV Test | |
|---|---|---|---|---|---|---|---|---|---|---|
| **Restraint** | BRS | DPS(ms) | BRS | DPS(ms) | BRS | DPS (ms) | BRS | DPS (ms) | BRS | DPS(ms) |
| Case #1 | 1.48 | 1 | 1.56 | -2 | 1.51 | -2 | 1.54 | -1 | 1.54 | -5 |
| Case #2 | 1.34 | -1 | 1.18 | -3 | 2.03 | -2 | 1.80 | 0 | 1.64 | -4 |
| Case #3 | 2.13 | 0 | 2.28 | -2 | 2.29 | 1 | 2.08 | 0 | 1.29 | -4 |
| Case #4 | 2.56 | 1 | 2.02 | -2 | 2.55 | 0 | 2.32 | 2 | 1.32 | -3 |
| **Average** | **1.88** | **0** | **1.76** | **-2** | **2.09** | **-1** | **1.93** | **0** | **1.45** | **-4** |

**Table 12**
**The average kinematics BRS scores of the GHBMC, THUMS, THOR, and THOR-AV models, and the THOR-AV test**

| | GHBMC | | THUMS | | THOR FE | | THOR-AV FE | | THOR-AV Test | |
|---|---|---|---|---|---|---|---|---|---|---|
| **HBM/ATD** | BRS | DPS(ms) | BRS | DPS(ms) | BRS | DPS(ms) | BRS | DPS(ms) | BRS | DPS(ms) |
| Case #1 | 0.84 | 1 | 0.72 | 1 | 0.61 | 2 | 0.70 | 0 | 0.84 | 3 |
| Case #2 | 0.93 | 3 | 0.83 | 0 | 0.71 | 0 | 0.84 | 0 | 0.77 | -3 |
| Case #3 | 0.94 | -1 | 1.06 | 0 | 1.26 | -1 | 0.87 | 0 | 0.73 | 0 |
| Case #4 | 1.28 | 0 | 1.45 | -1 | 1.36 | -1 | 1.12 | 0 | 0.89 | -1 |
| **Average** | **1.00** | **1** | **1.01** | **0** | **0.98** | **0** | **0.88** | **0** | **0.81** | **0** |

# DISCUSSION

In general, the kinematics of all four FE models matched their PMHS counterpart reasonably well; evidenced by their BRS scores. However, the occupant-to-restraint interaction requires improvement.

The restraint system used for test series 2 (Case #3 and #4) simulations did not include a dynamic locking tongue. The authors were made aware that a 2 kN dynamic locking tongue was used in the corresponding PMHS tests when writing this manuscript. The authors reviewed the shoulder belt and lap belt loads time history and found that the belt loads of the simulations matched the outputs of the PMHS tests reasonably well. The shoulder belt payout of the FE simulations also matched the PMHS results reasonably well. Based on this analysis, the authors do not believe the simulation outputs were compromised due to the lack of a dynamic locking tongue.

The seat force in the z-direction was higher than the PMHS results in Case #1 (Figure A6) and #3 (Figure A17) for all four occupant models. The PMHS mass (average of 68.1 kg with a range of 53.0 to 80.3 kg) used to derive the PMHS corridors was much lower than the mass of an average male (76.8 kg). This mass-mismatch may have contributed to the lower seat force in the z-direction for PMHS corridors. Normalization of the PMHS test data could reduce this force discrepancy and improve the BRS scores for the FE occupants.

It was noticed that the anti-submarining plate rotations were significantly higher for the FE models in Case #3 and #4 (Figure A19). In physical dummy tests, it was observed that the rotations of the seat pan and the anti-submarining plate did not correlate well with the PMHS responses [10][11]. The causes were not very clear and is worthy of further investigation.

The lap belt force of the four FE models matched that of the PMHSs reasonably well in Case #1 and #2 (Figure A1 through Figure A4). However, the lap belt force of the GHBMC and THUMS models in Case #3 and #4 were higher than the PMHS results (Figure A20 and Figure A21), while the shoulder belt force for all four FE models matched the PMHS results reasonably well. The results did not give a clear direction for future optimization of the FE models. To understand the issue better, the pelvis flesh stiffness was investigated to understand the lap belt engagement with the pelvis using the UMTRI simulations (Case #3 and #4). The investigation focused on the belt forces and pelvis hip displacement relationship, which was expected to be a reasonable indicator of the stiffness of the flesh in front of the ASIS. Since the buckle side load cell measured the sum of the shoulder belt and lap belt forces, the force for the lap belt alone on the buckle side cannot be segregated. Therefore, the outboard lap belt force was doubled for this analysis. As shown in Figure 8, the stiffnesses of the pelvis flesh (slope of lap belt force vs. hip displacement) for the GHBMC, THUMS, THOR, and THOR-AV models are comparable to the stiffnesses of pelvis flesh for the PMHS.

The body mass and stature of the PMHS specimens varied from 53 kg to 80.3 kg and 166.3 cm to 175.7 cm respectively, for the UMTRI tests. The specimens that best matched the average male weight and height were the PMHS 2104 (body mass 80.3 kg, stature 170.1 cm) in the 25° seatback test condition, and the PMHS 2002 (body mass 76.1 kg, stature 174.9 cm) in the 45° seatback test condition. For the belt force vs hip displacement responses, both the THOR and THOR-AV models showed comparable results to these PMHS tests respectively in each test configuration. The GHBMC and THUMS models matched the stiffer responses of the PMHSs, shown in Figure 8.

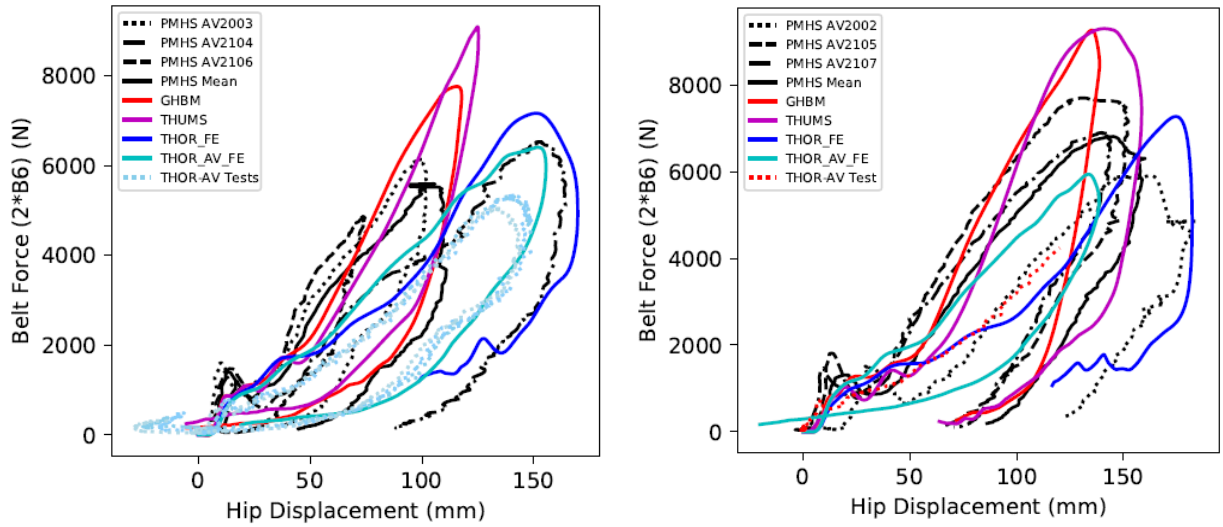


Figure 8. Belt force vs hip displacement in the 25° (left) and 45° (right) UMTRI test configurations

The GHBMC, THUMS, THOR, and THOR-AV restraint system biofidelity was notably worse than the kinematics biofidelity (Table 11 and Table 12), and should be investigated in the future.

In the front- and rear-seat test configurations (Case #1 and #2), the pelvis rotations matched the PMHS response well (Figure A11). For the UMTRI 25° test condition (Case #3), the pelvis y-rotation fell within the PMHS corridor for all models; the THOR model near the upper bound and THOR-AV and THUMS models near the lower bound (Figure A41). For the 45° recline condition (Case #4), the pelvis rotation for the GHBMC and THOR-AV models fell out of (i.e. below) the lower bound, while the THUMS model was near the upper bound and the THOR model was in the middle. It was noted the pelvis rotation in y-direction was opposite to PMHS pelvis rotation observed in Richardson et al. study [18], most probably explained by the difference in restraint system and impact pulse. Also, the UMTRI test used a 32 km/h delta velocity and no lap belt pretensioner, versus a 50 km/h and dual lap belt pretensioner in Richardson et al.

## LIMITATIONS

No effort was made to improve the biofidelity of the four FE models in the current study. As presented in this paper, the THOR-AV physical dummy test results had slightly better biofidelity than the THOR-AV FE model (v0.6). This will be addressed by Humanetics in the next release. As mentioned in the discussion, a dynamic locking tongue was not simulated in Case #3 and 4, even though one was used in the physical tests. Since the shoulder belt payout and shoulder belt loads were comparable between the simulations and the PMHS tests, the authors do not believe there was a negative effect on the results.

## CONCLUSIONS

The biofidelity of the GHBMC, THUMS, THOR, and THOR-AV models was evaluated in four test configurations. Using the NHTSA BioRank method, the four FE occupant models demonstrated *good* to *excellent* kinematic biofidelity as compared to PMHSs. The restraint system BioRank scores were not as good as the models' kinematic responses; however, except for the THOR model, they were ranked as *good*. The interaction between all four occupant models and the restraint system needs improvement. The THOR-AV FE model was modified to match the human hip joint height, improving its seated height, and potentially the submarining responses of the dummy. The stiffness in front of the ASIS appeared to be reasonable when comparing with the PMHS results under lap belt loading condition. It was also observed that the HBM responses were comparable to the ATD responses for all test configurations.

## ACKNOWLEDGEMENT

The AVOS Consortium would like to express its gratitude for the support of the consortium member companies. The views expressed in this manuscript are those of the consortium's individual participants and may not represent the views of their respective organizations.

For any questions related to this paper, please contact the lead author, Z. Jerry Wang, Ph.D., Tel +1 248 778 2133, Email jwang@humaneticsatd.com, Humanetics Innovative Solutions, Inc., 23300 Haggerty Road, Farmington Hills, Michigan 48335, USA. Humanetics Innovative Solutions is the host company of the AVOS Consortium.

## REFERENCES

[1] Leung Y.C., Terriere C., Fayon, A., Mairesse P., Delmas A., Banzet P., A comparison between part 572 dummy and human subject in the problem of submarining, 23rd Stapp Car Crash Conference, October 1979.

[2] Uriot J., Baudrit P., Portier P., Trosseille X., Petit P., Guillemot H., Guerin L., Vallancien G. Investigation on the belt-to-pelvis interaction in case of submarining. Stapp Car Crash Journal, Vol. 50 (Nov 2006), pp.53-73.

[3] Uriot, J, Potier, P, Baudrit, P, Trosseille, X, Richard, O. and Douard, R, Comparison of HII, HIII and THOR dummy responses with respect to PMHS sled tests, IRCOBI Conference Proceedings, Lyon France, Sept 9-11, 2015.

[4] Richardson R., Donlon J.P., Jayathirtha M., Forman J.L., Shaw G., Gepner B., Kerrigan J.R., Östling M., Mroz K., Pipkorn B., Kinematics and injury response of reclined PMHS in frontal impacts, Stapp Car Crash Journal, Vol. 64, November 2020.

[5] Richardson R., Jayathirtha M., Donlon J.P., Forman J.L., Gepner B., Östling M., Mroz K., Pipkorn B., Kerrigan J.R., Pelvis kinematics and injuries of reclined occupants in frontal impacts, IRCOBI, 2020.

[6] Gepner B.D., Draper D., Mroz K., Richardson R., Östling M., Pipkorn B., Forman J. L., Kerrigan J. R. 2019. Comparison of human body models in frontal crashes with reclined seatback. 2019. IRCOBI Conference Proceedings, September 11-13, 2019, Florence, Italy.

[7] Mroz K., Östling M, Richardson R, Kerrigan K, Forman J, Gepner B, Lubbe N, Pipkorn B, 2020. Effect of seat belt characteristics on the lumbar spine and pelvis loading of the SAFER Human Body Model in reclined postures, IRCOBI, 2020 (virtual).

[8] Östh J. Bohman K., Jakobsson L., Evaluation of kinematics and restraint interaction with repositioning a driver from a reclined to an upright position prior to frontal impact using active human body model simulations, IRCOBI conference, 2020.

[9] NHTSA test report, NHTSA Biomechanics Database, September 20, 2020, test # b12795, https://nrd-static.nhtsa.dot.gov/reports/biodb/b10000/b12700/b12795R005.pdf and January 25th, 2021, test # b13109 https://nrd-static.nhtsa.dot.gov/reports/biodb/b10000/b13100/b13109R001.pdf,

[10] Wang Z.J., Richard O., Lebarbé M. Uriot J., Kabadayi E., Kleessen C., Biomechanical responses of THOR-AV in a semi-rigid seat that mimicked the front and rear seat, IRCOBI conference, Porto, Portugal, September 14-16, 2022.

[11] Wang Z.J., Zaseck L.W., Reed M.P., THOR-AV 50th percentile male biofidelity evaluation in 25 and 45 seatback angle test conditions with a semi-rigid seat, IRCOBI conference, Porto, Portugal, September 14-16, 2022.

[12] Rhule H.R., Maltese M.P., Donnelly B.R., Eppinger R.H., Brunner J.K. and Bolte IV J.H., Development of a new biofidelity ranking system for anthropomorphic test devices, Stapp Car Crash Journal, 46th Stapp Car Crash Conference, November 2002.

[13] Rhule H., Moorhouse K., Donnelly B., Stricklin J., Comparison of WorldSID and ES-2RE biofidelity using an updated biofidelity ranking system, 21st International Technical Conference on Enhanced Safety of Vehicles (ESV), Stuttgart, Germany, June 2009.

[14] Rhule H., Donnelly B., Moorhouse K., Kang Y-S., A methodology for generating objective target for quantitively assessing the biofidelity of crash test dummies, 23rd International Technical Conference on Enhanced Safety of Vehicles (ESV), Seoul, Korea, May 27-30, 2013.

[15] Rhule H., Stricklin J., Moorhouse K., Donnelly B., Improvements to NHTSA's biofidelity ranking system and application to the evaluation of the THOR 5th female dummy, IRCOBI Conference Proceedings, 2018, paper # IRC-18-12.

[16] Kang Y-S., Stammen J., Ramachandra R., Agnew R.M. Hagedorn, A., Thomas C., Kwon H.J., Moorhouse K., Bolte IV J.H., Biomechanical responses and injury assessment of post-mortem human subjects in various rear-facing seating configurations. Stapp Car Crash Journal, vol. 64 (November 2020), pp. 155-212.

[17] Schneider, L.W., Robbins, D.H., Pflug, M.A., Snyder, R.G., 1983. Anthropometric specifications for mid-sized male dummy, Vol. 2, UMTRI-83-53-2.

[18] Richardson R., Donlon J.P., Jayathirtha M., Forman J.L., Shaw G., Gepner B., Kerrigan J.R., Östling M., Mroz K., Pipkorn B., Kinematics and injury response of reclined PMHS in frontal impacts, Stapp Car Crash Journal, Vol. 64 (November 2020).

## APPENDIX

The overlay of the channels from GHBMC, THUMS, THOR, and THOR-AV FE models are shown in this appendix for all four cases.

**Plots for the front- and rear-seat test configurations (Case #1 and #2)**

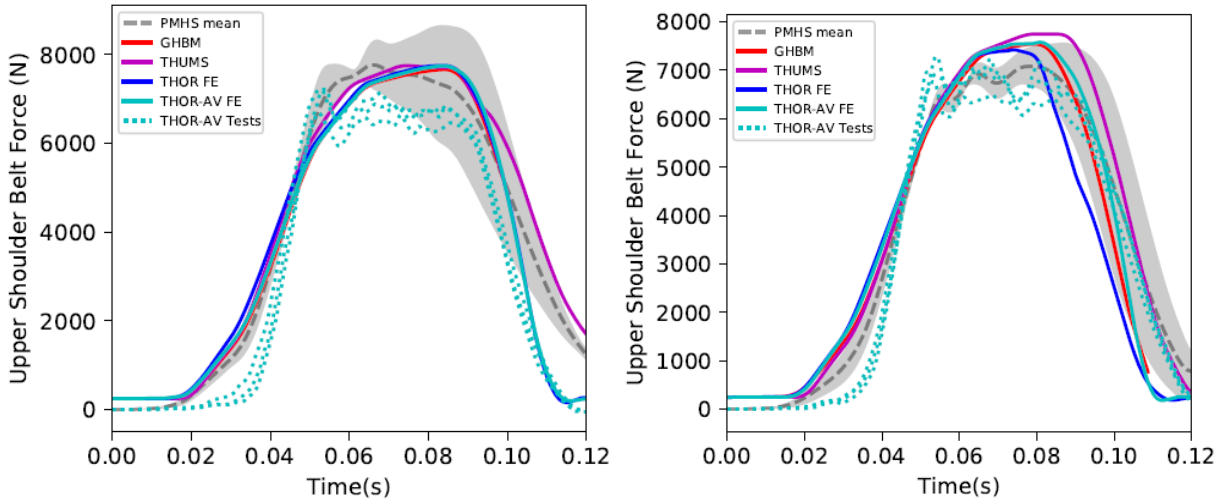


Figure A1. Upper shoulder belt force in the front-seat (Case #1, left) and the rear-seat (Case #2, right) test configurations.

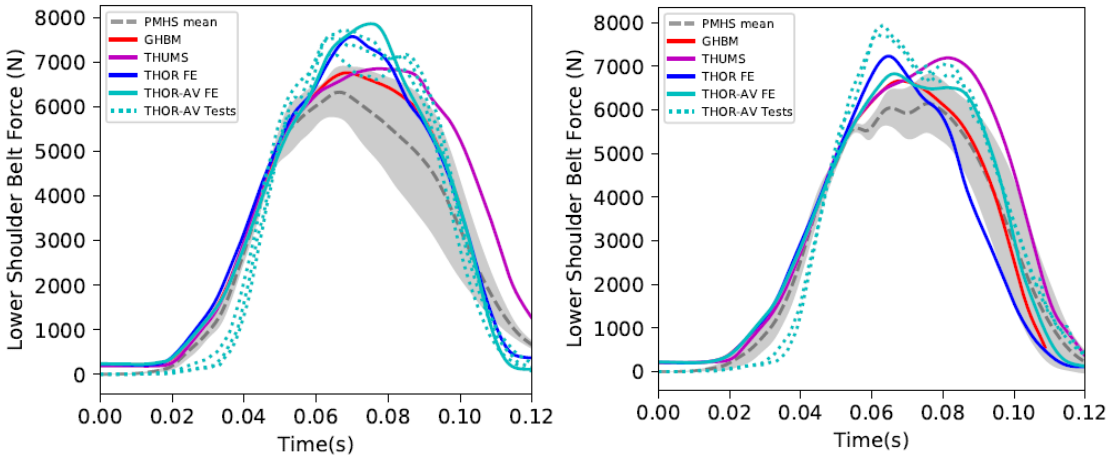


Figure A2. Lower shoulder belt force in the front-seat (Case #1, left) and the rear-seat (Case #2, right) test configurations.

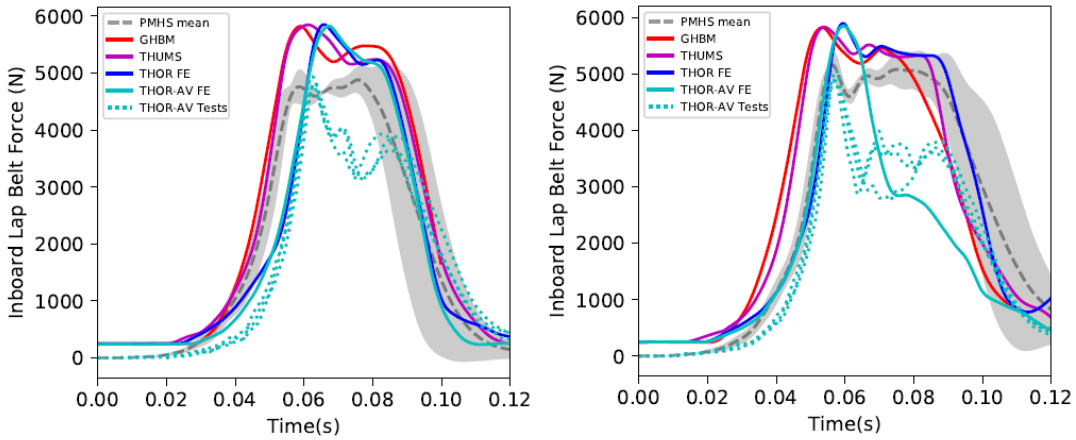


Figure A3. Inboard lap belt force in the front-seat (Case #1, left) and the rear-seat (Case #2, right) test configurations.

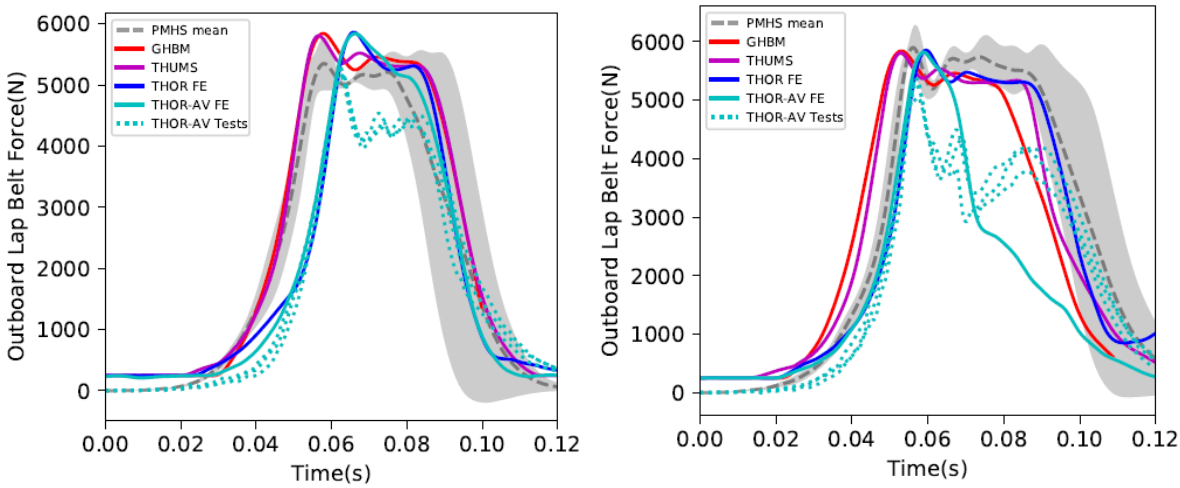


Figure A4. Outboard lap belt force in the front-seat (Case #1, left) and the rear-seat (Case #2, right) test configurations.

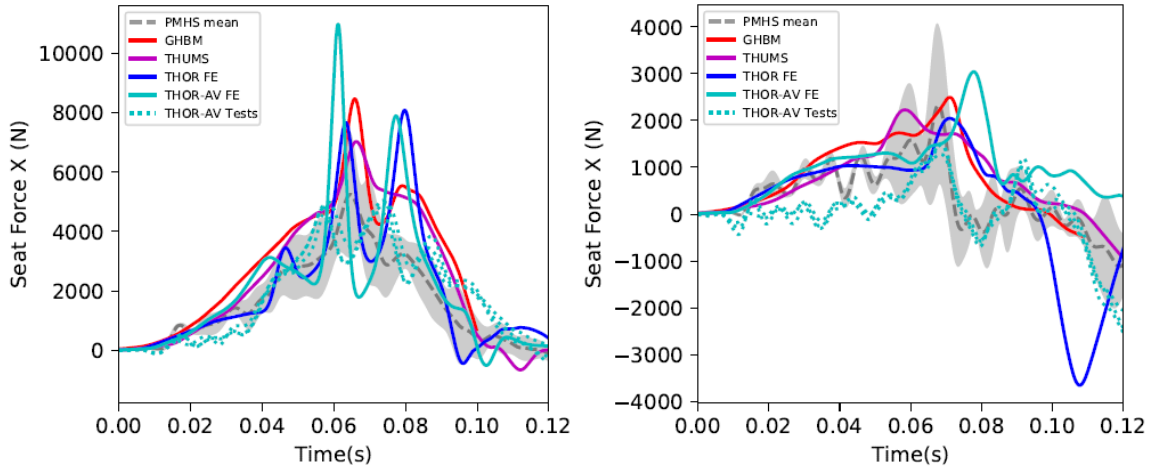


Figure A5. Seat force X in the front-seat (Case #1, left) and the rear-seat (Case #2, right) test configurations.

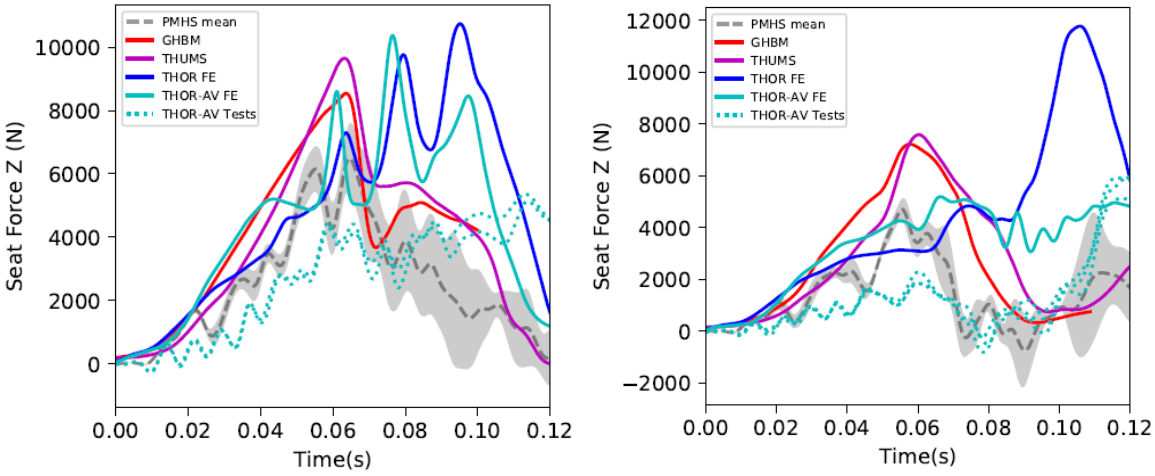


Figure A6. Seat force Z in the front-seat (Case #1, left) and the rear-seat (Case #2, right) test configurations

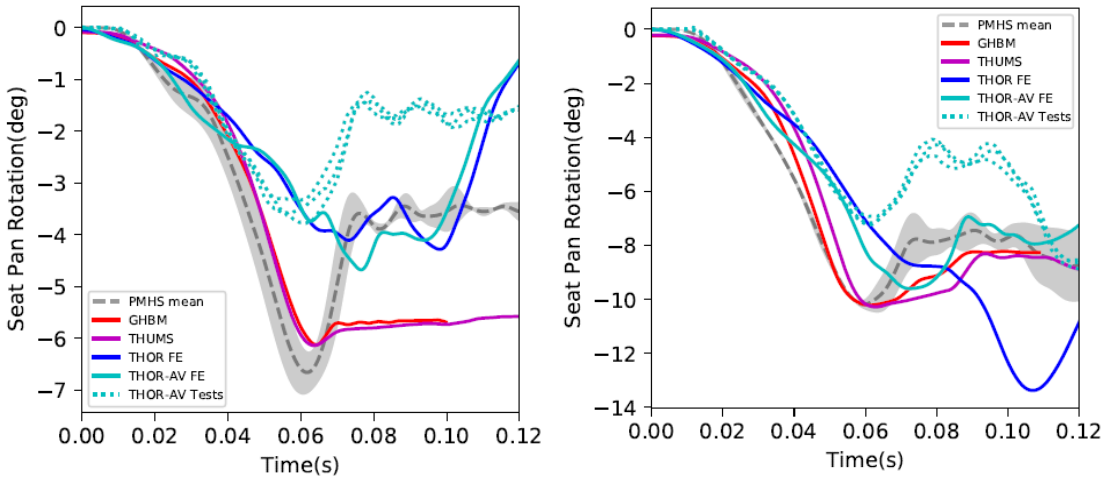


Figure A7. Seat pan rotation in the front-seat (Case #1, left) and the rear-seat (Case #2, right) test configurations.

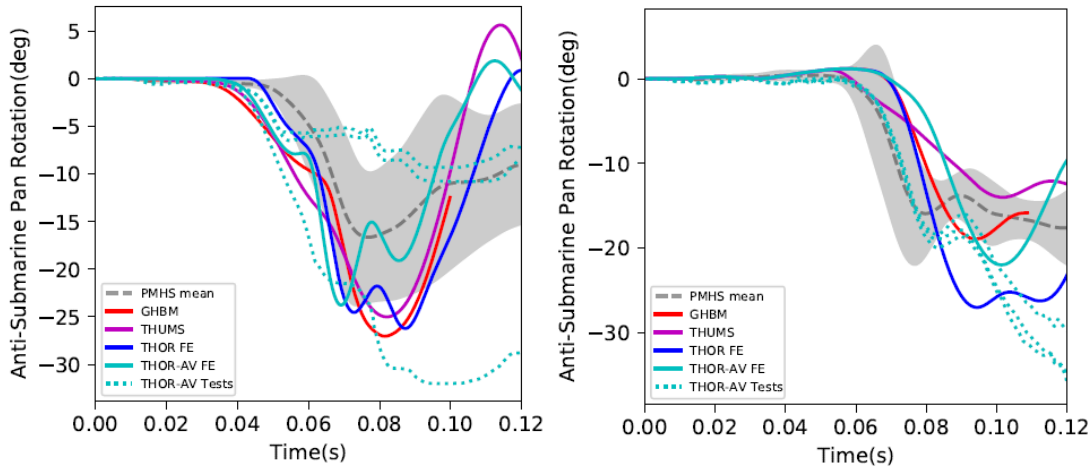


Figure A8. Anti-submarine plate rotation in the front-seat (left) and the rear-seat (right) test configurations.

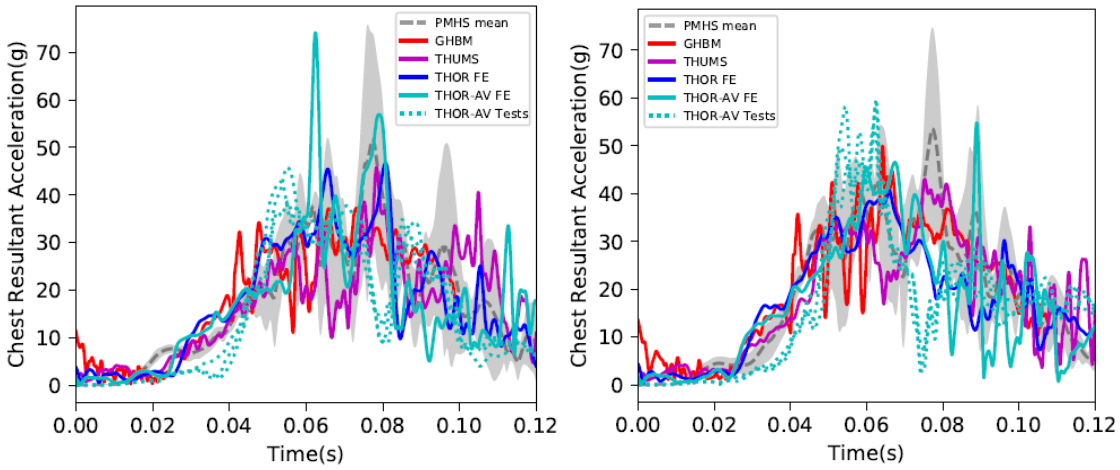


Figure A9. Chest resultant acceleration in the front-seat (Case #1, left) and rear-seat (Case #2, right) test configurations.

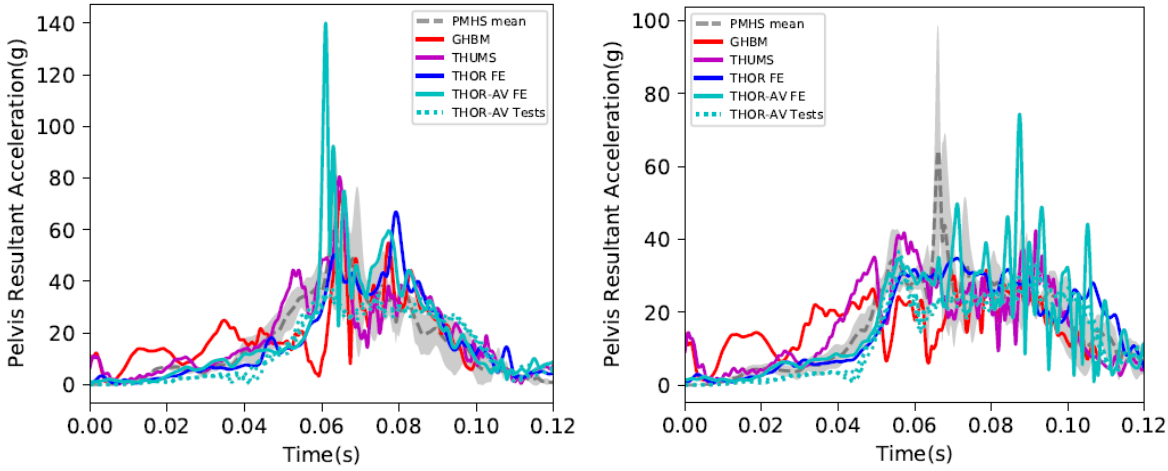


Figure A10. Pelvis resultant acceleration in the front-seat (Case #1, left) and the rear-seat (Case #2, right) test configurations.

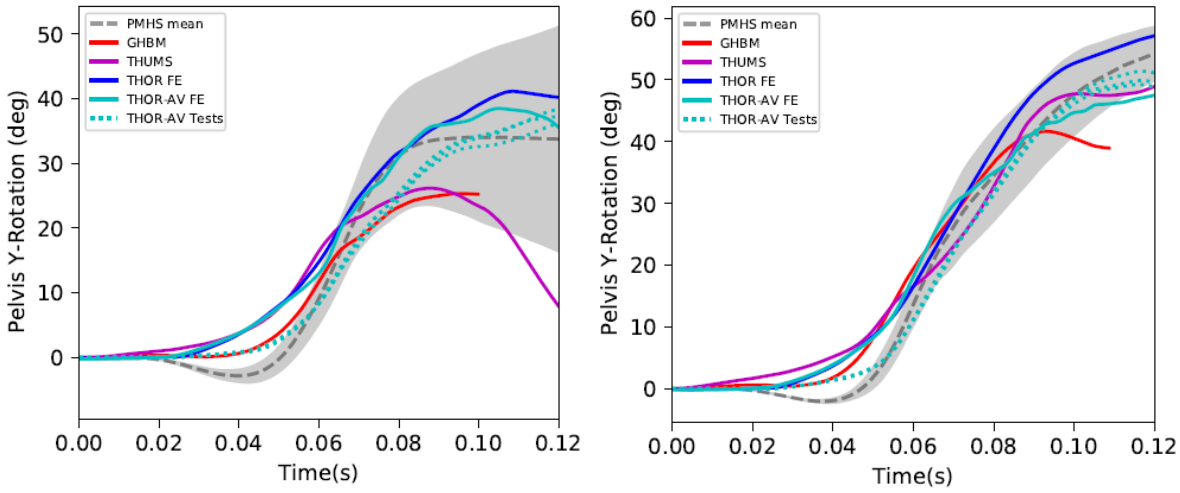


Figure A11. Pelvis y-rotation in the front-seat (Case #1, left) and the rear-seat (Case #2, right) test configurations.

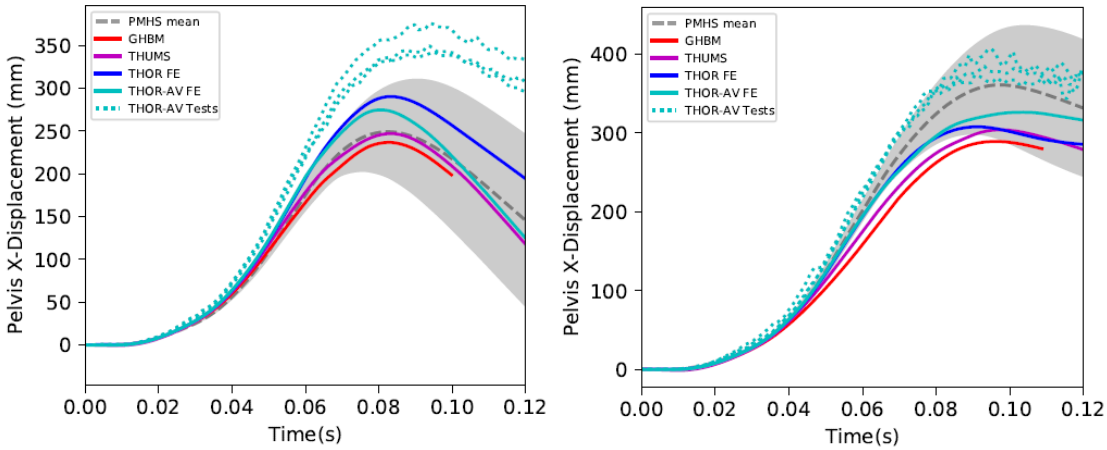


Figure A12. Pelvis x-displacement in the front-seat (Case #1, left) and rear-seat (Case #2, right) test configurations.

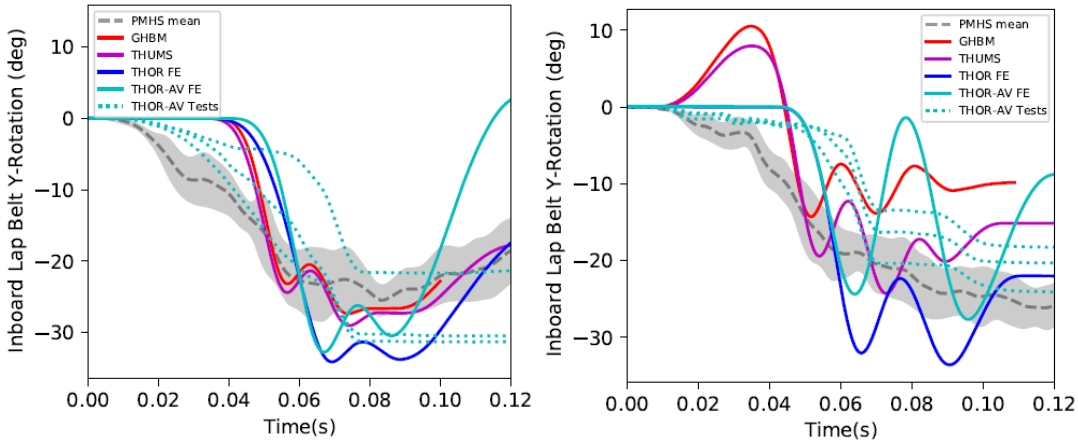


Figure A13. Inboard lap belt y-rotation in the front-seat (Case #1, left) and the rear-seat (Case #2, right) test configurations.

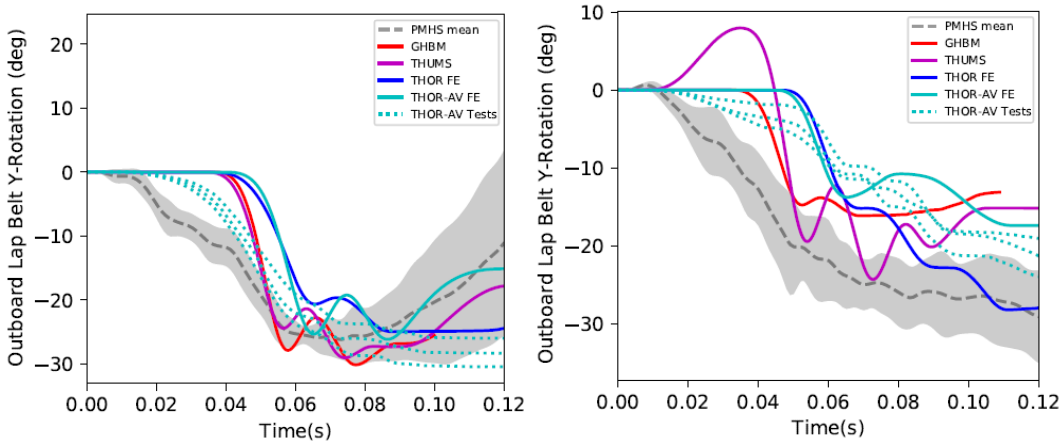


Figure A14. Outboard lap belt y-rotation in the front-seat (Case #1, left) and the rear-seat (Case #2, right) test configurations.

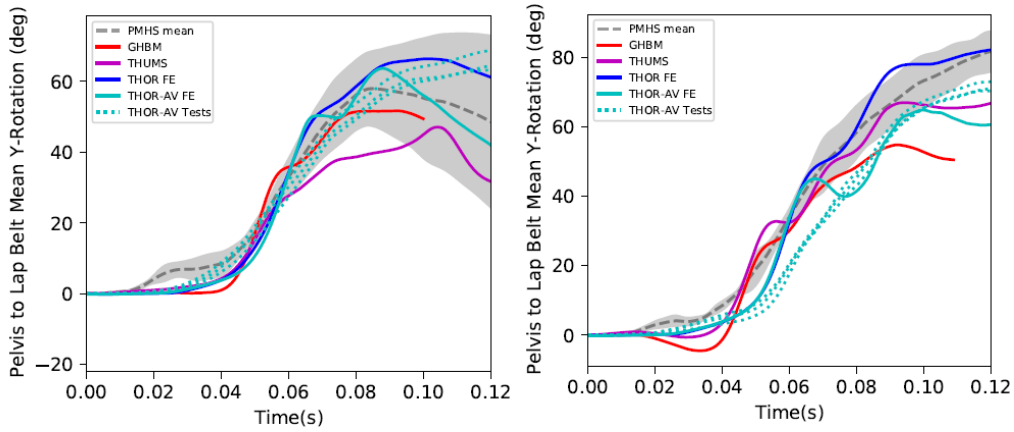


Figure A15. Pelvis to lap belt mean relative y-rotation in the front-seat (Case #1, left) and rear-seat (Case #2, right) test configurations.

**Plots for the UMTRI 25° and 45° test configurations (Case #3 and #4)**

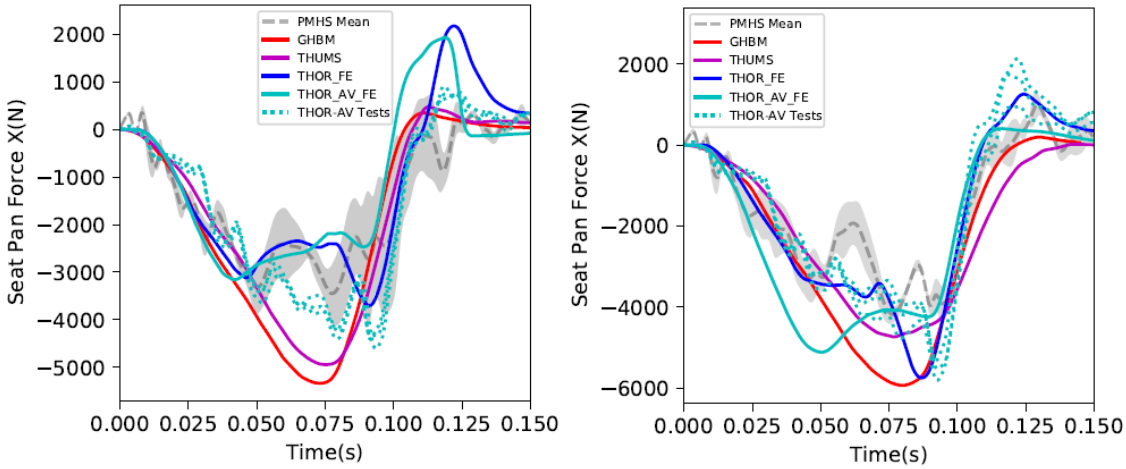


Figure A16. Seat pan force X in 25° (Case #3, left) and 45° (Case #4, right) seatback UMTRI test configurations.

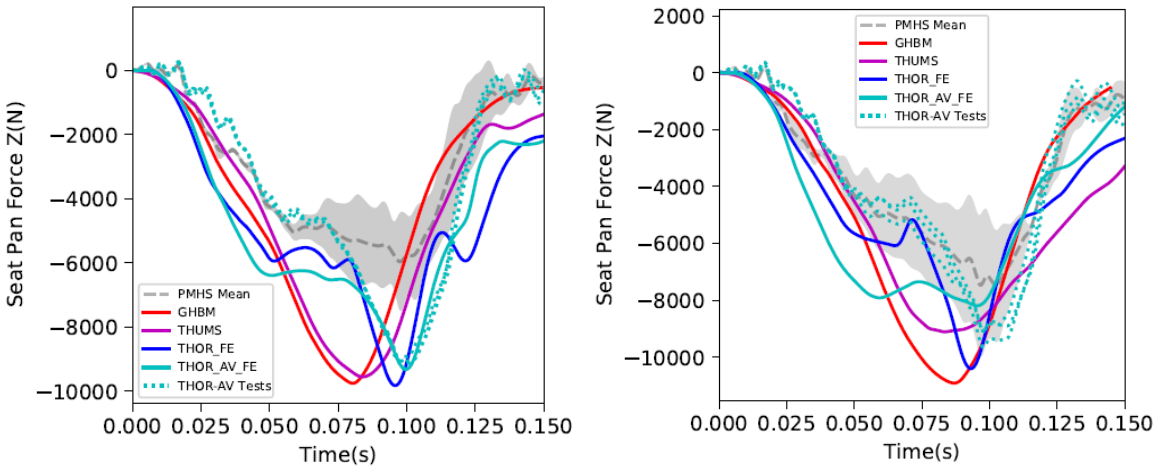


Figure A17. Seat pan force Z in 25° (Case #3, left) and 45° (Case #4, right) seatback UMTRI test configurations.

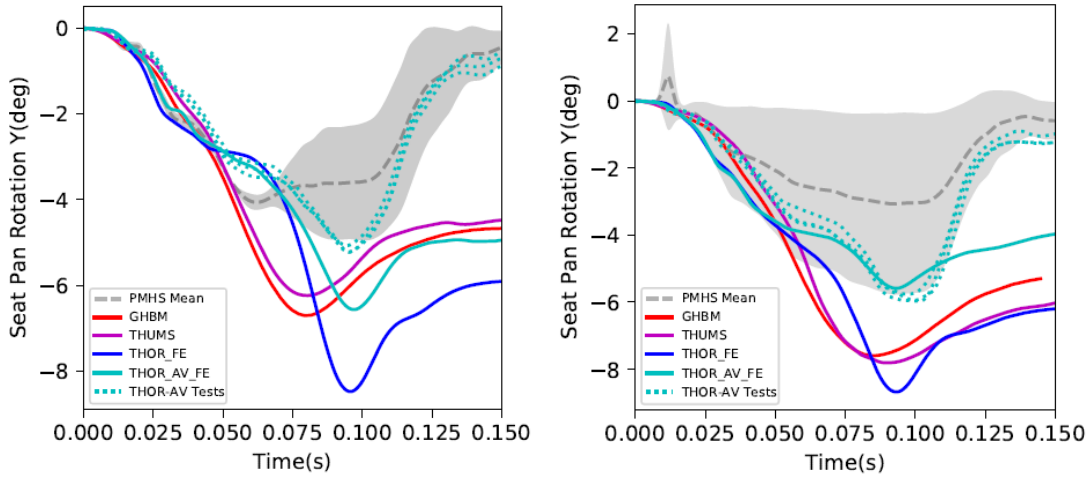


Figure A18. Seat pan rotation Y in 25° (Case #3, left) and 45° (Case #4, right) seatback UMTRI test configurations.

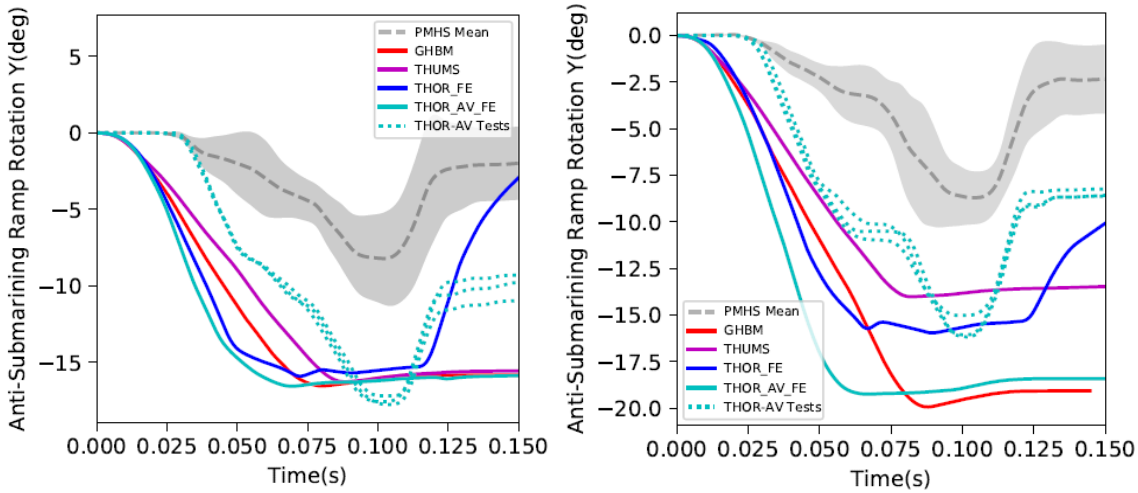


Figure A19. Anti-submarining ramp rotation in 25° (Case #3, left) and 45° (Case #4, right) seatback UMTRI test configurations.

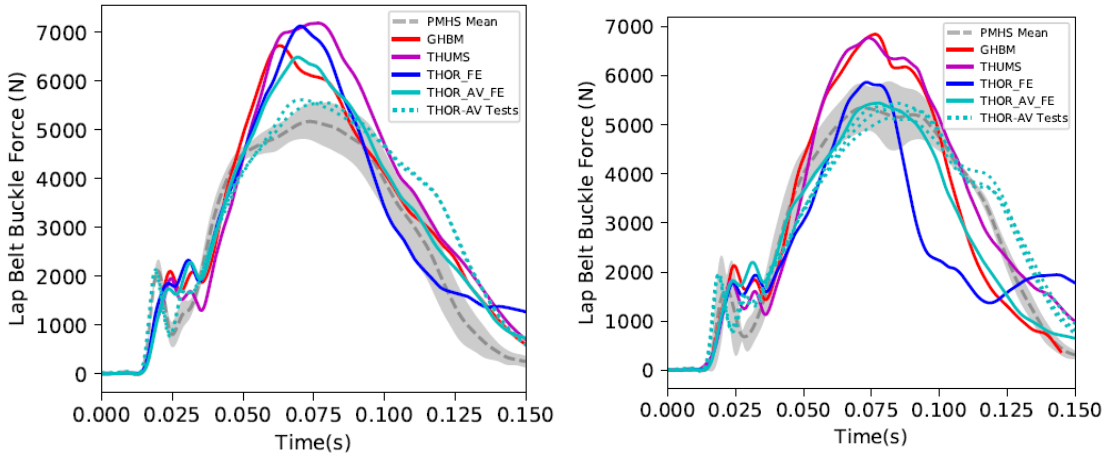


Figure A20. Buckle force in 25° (Case #3, left) and 45° (Case #4, right) seatback UMTRI test configurations.

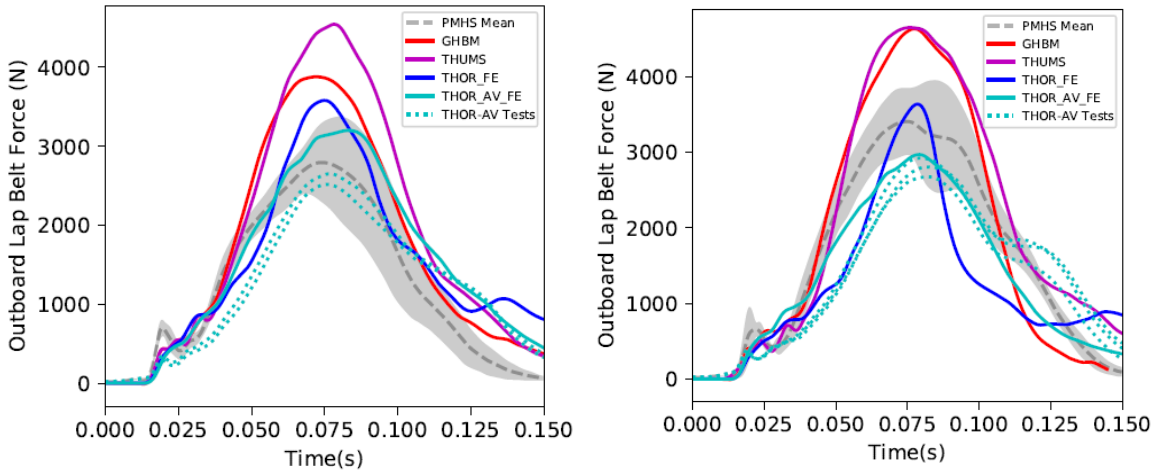


Figure A21. Outboard lap belt force in 25° (Case #3, left) and 45° (Case #4, right) seatback UMTRI test configurations.

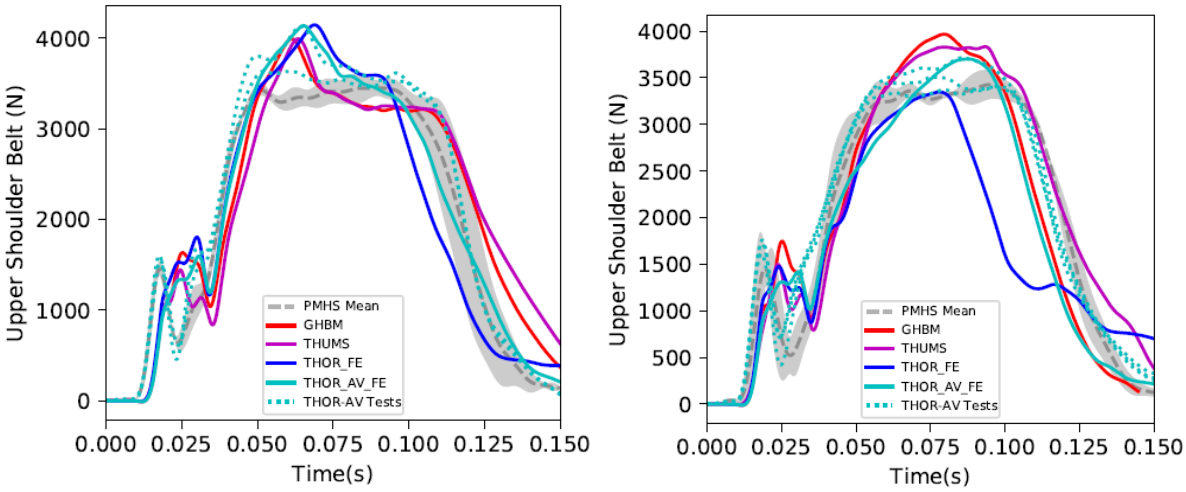


Figure A22. Upper shoulder belt force in 25° (Case #3, left) and 45° (Case #4, right) seatback UMTRI test configurations.

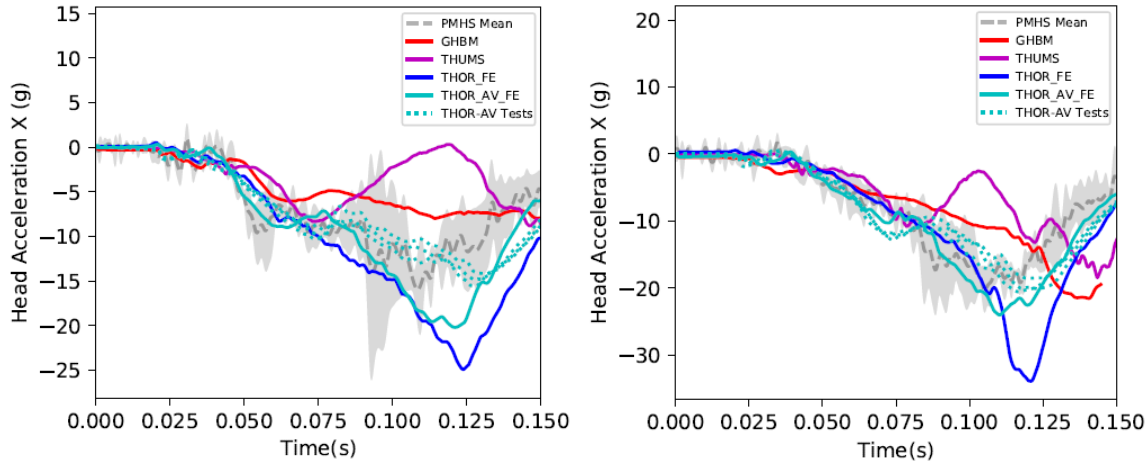


Figure A23. Head acceleration X in 25° (Case #3, left) and 45° (Case #4, right) seatback UMTRI test configurations

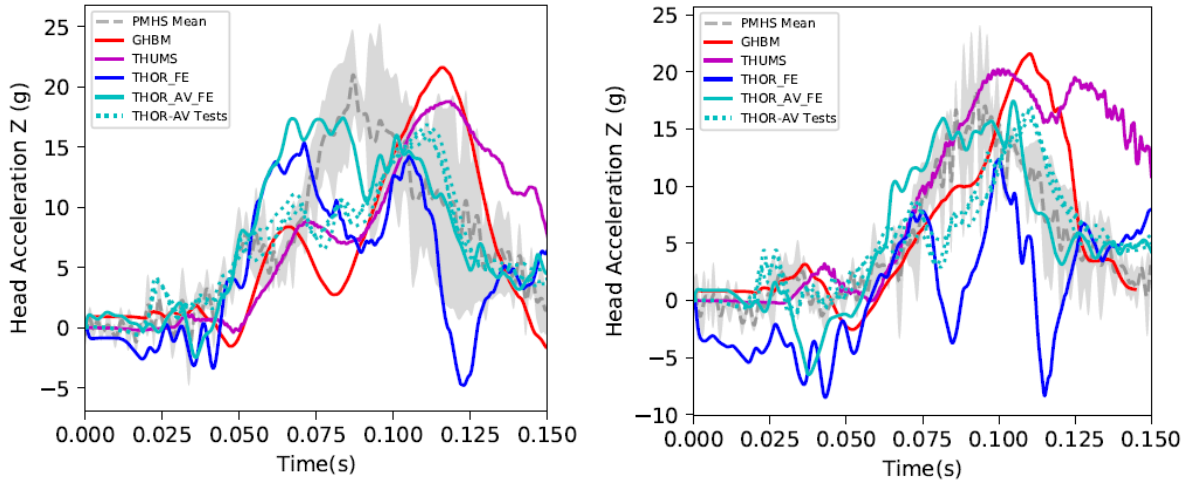


Figure A24. Head acceleration Z in 25° (Case #3, left) and 45° (Case #4, right) seatback UMTRI test configurations

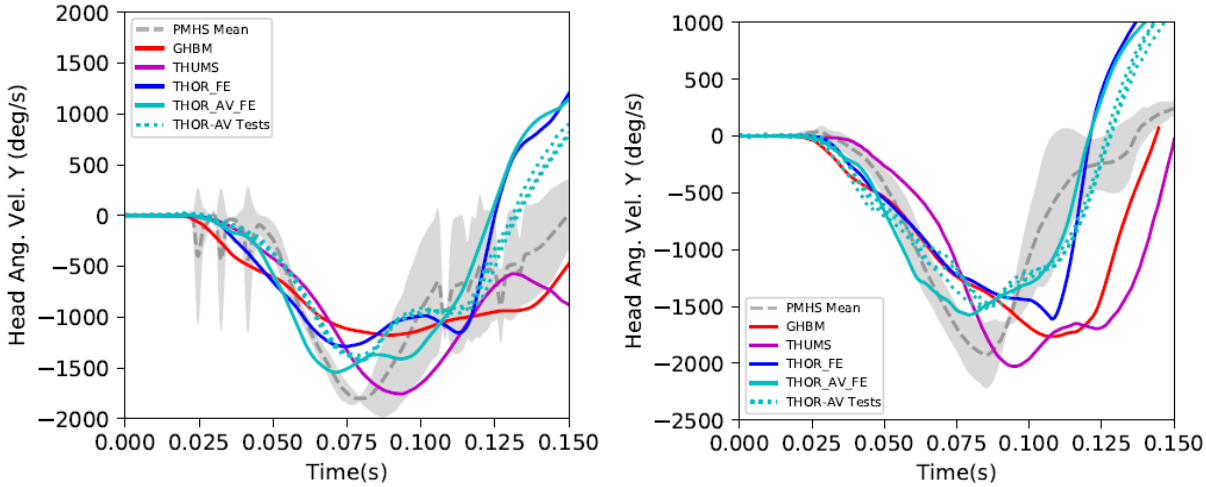


Figure A25. Head angular velocity Y in 25° (Case #3, left) and 45° (Case #4, right) seatback UMTRI test configurations

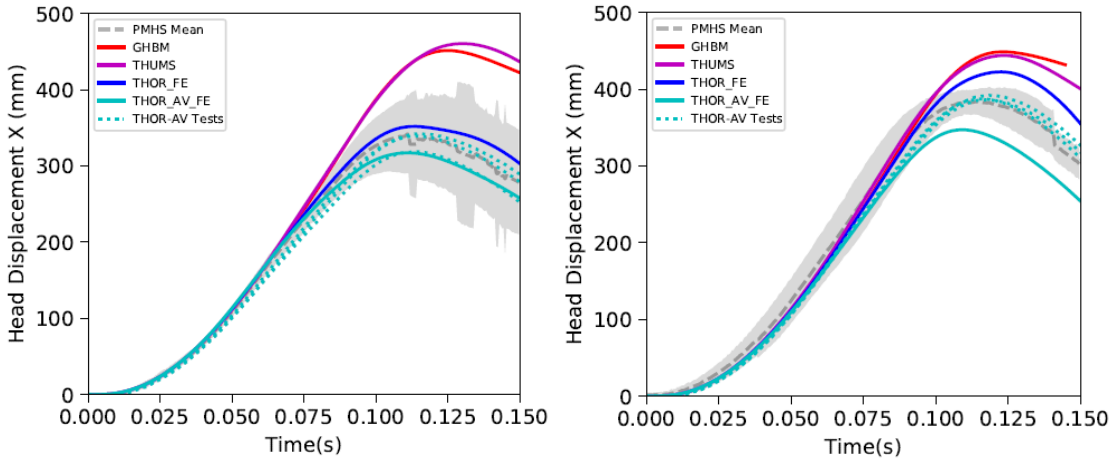


Figure A26. Head displacement X in 25° (Case #3, left) and 45° (Case #4, right) seatback UMTRI test configurations

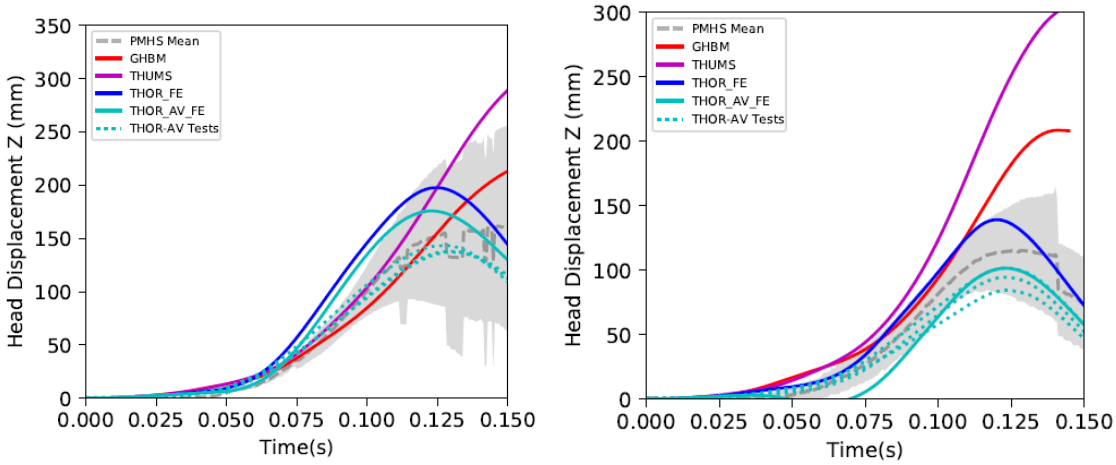


Figure A 27. Head displacement Z in 25° (Case #3, left) and 45° (Case #4, right) seatback UMTRI test configurations

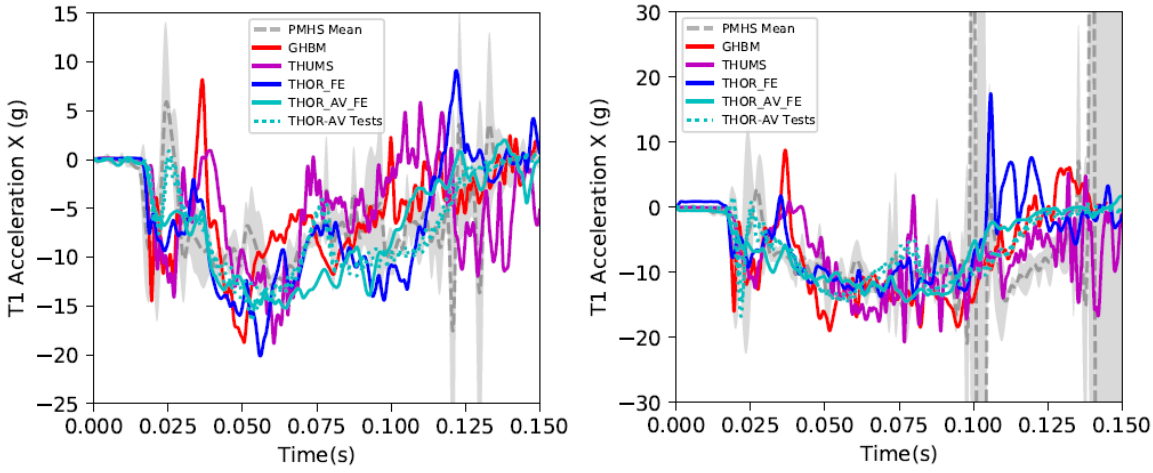


Figure A28. T1 acceleration X in 25° (Case #3, left) and 45° (Case #4, right) seatback UMTRI test configurations.

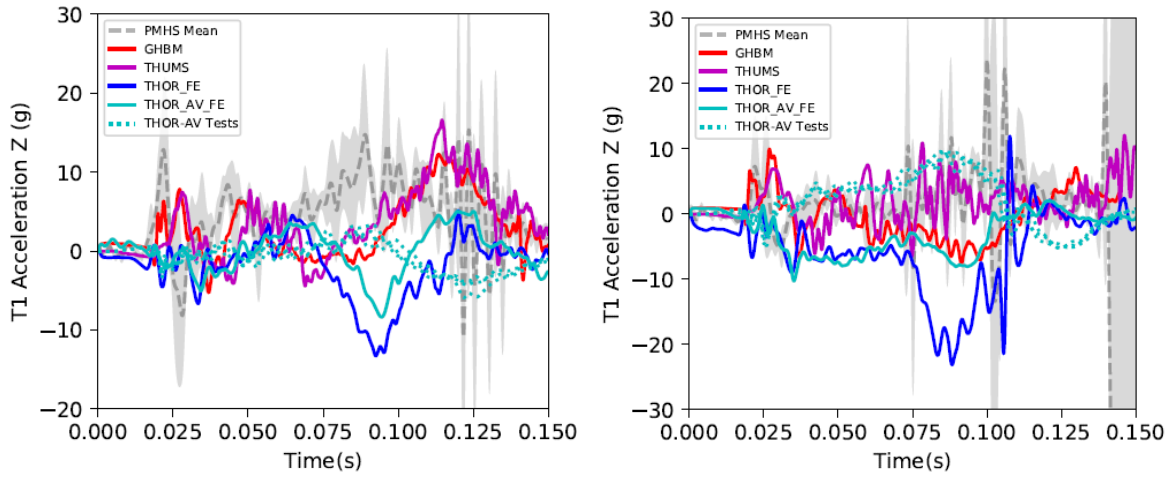


Figure A29. T1 acceleration Z in 25° (Case #3, left) and 45° (Case #4, right) seatback UMTRI test configurations.

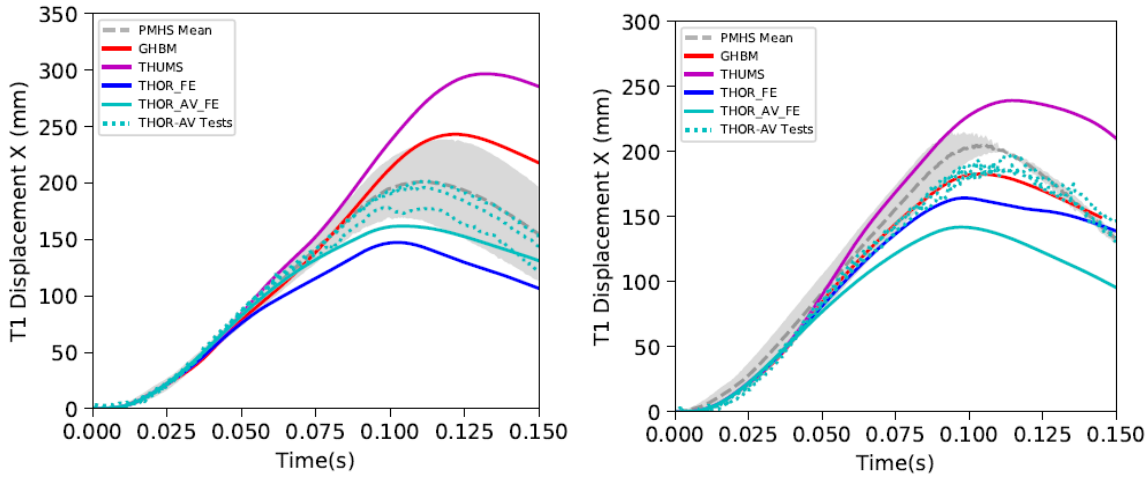


Figure A30. T1 displacement X in 25° (Case #3, left) and 45° (Case #4, right) seatback UMTRI test configurations.

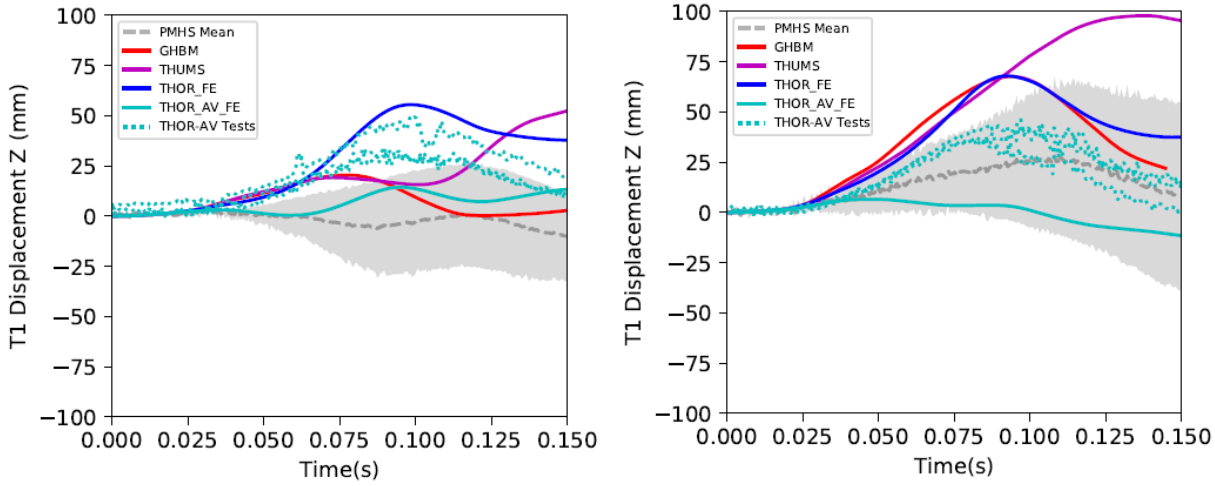


Figure A31. T1 displacement in Z in 25° (Case #3, left) and 45° (Case #4, right) seatback UMTRI test configurations

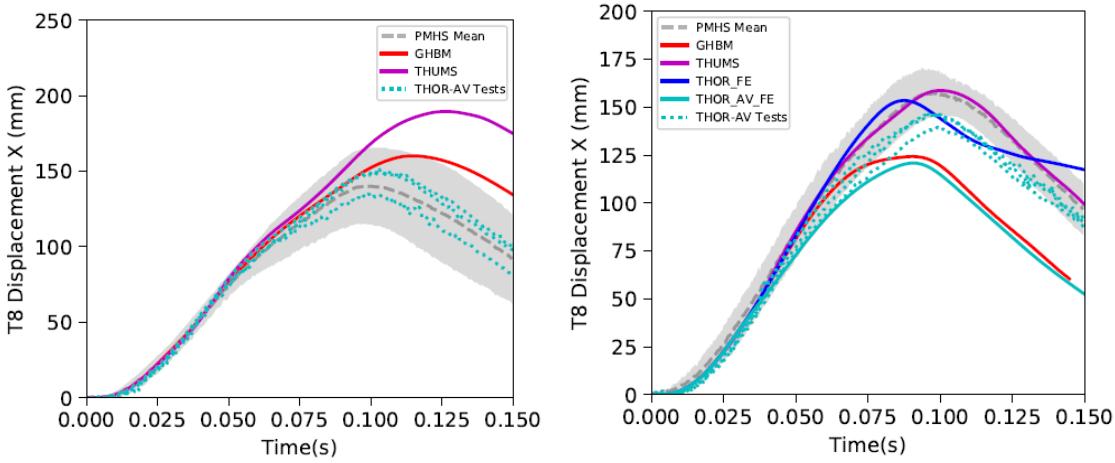


Figure A32. T8 displacement X in 25° (Case #3, left) and 45° (Case #4, right) seatback UMTRI test configurations.

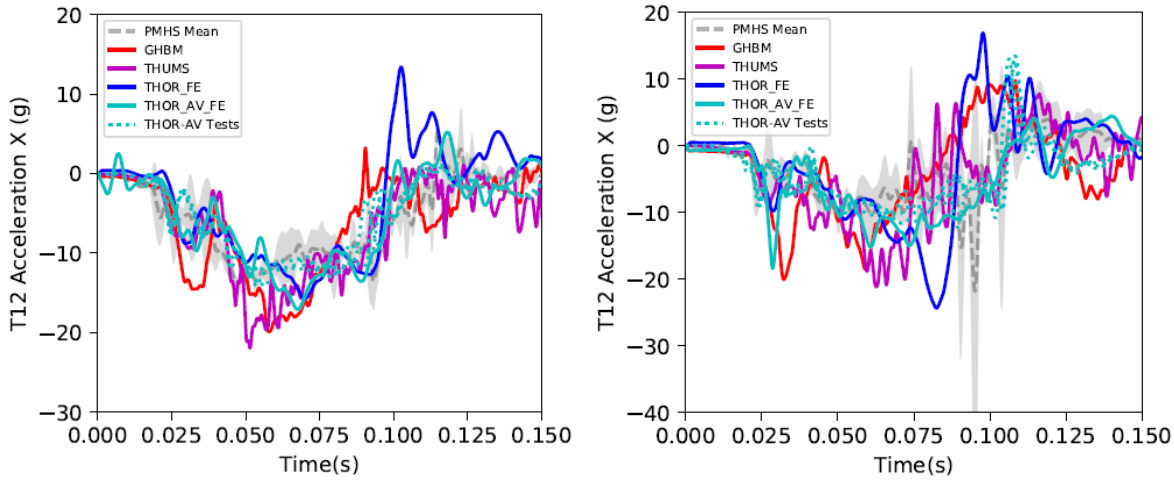


Figure A33. T12 acceleration X in 25° (Case #3, left) and 45° (Case #4, right) seatback UMTRI test configurations.

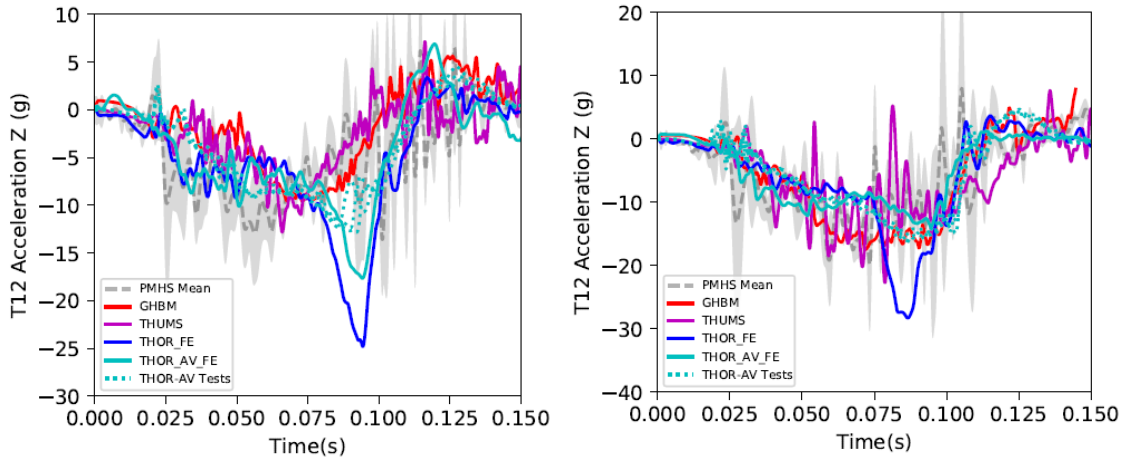


Figure A34. T12 acceleration Z in 25° (Case #3, left) and 45° (Case #4, right) seatback UMTRI test configurations

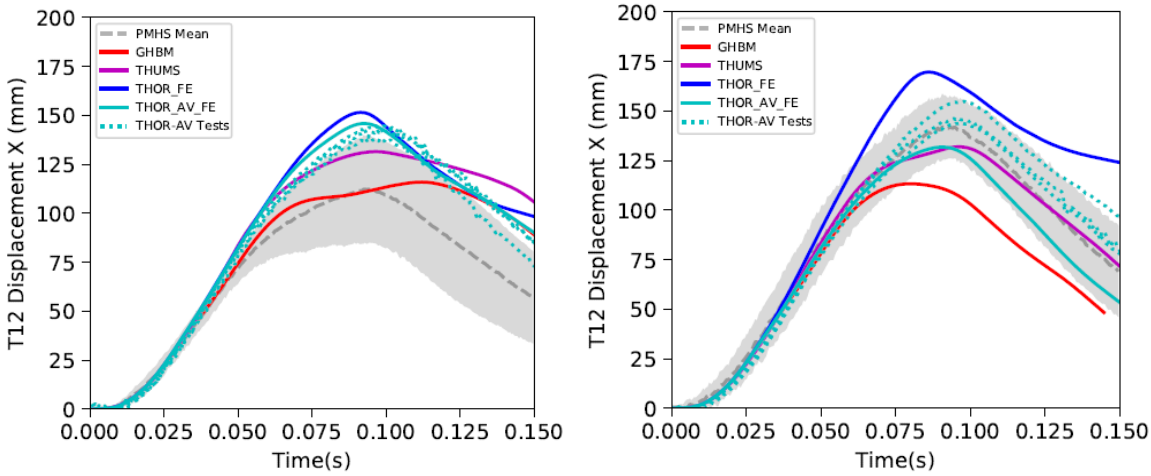


Figure A35. T12 displacement X in 25° (Case #3, left) and 45° (Case #4, right) seatback UMTRI test configurations

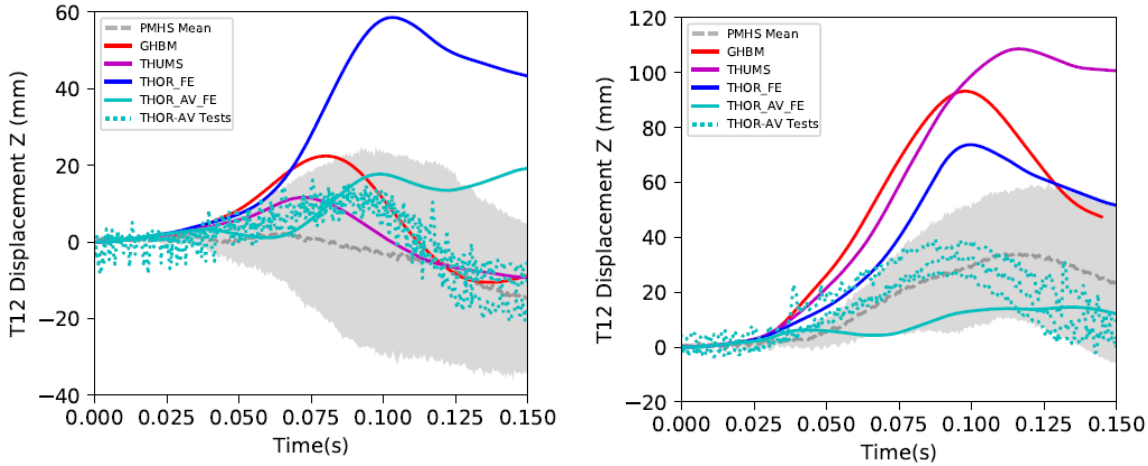


Figure A36. T12 displacement Z in 25° (Case #3, left) and 45° (Case #4, right) seatback UMTRI test configurations

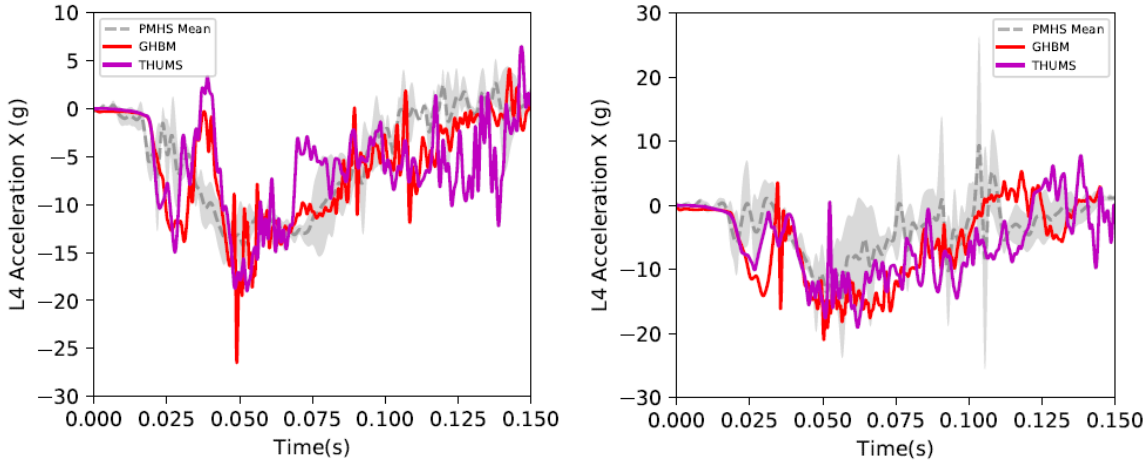


Figure A37. L4 acceleration X in 25° (Case #3, left) and 45° (Case #4, right) seatback UMTRI test configurations

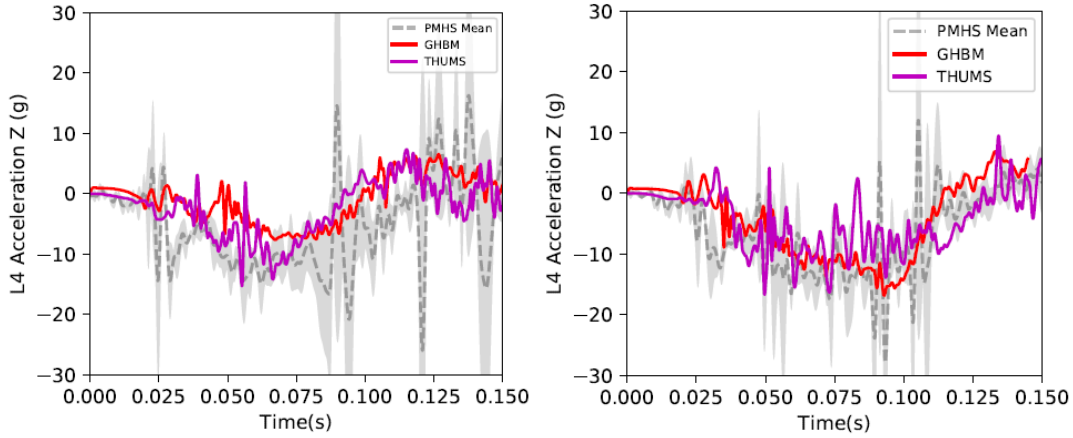


Figure A38. L4 acceleration Z in 25° (Case #3, left) and 45° (Case #4, right) seatback UMTRI test configurations

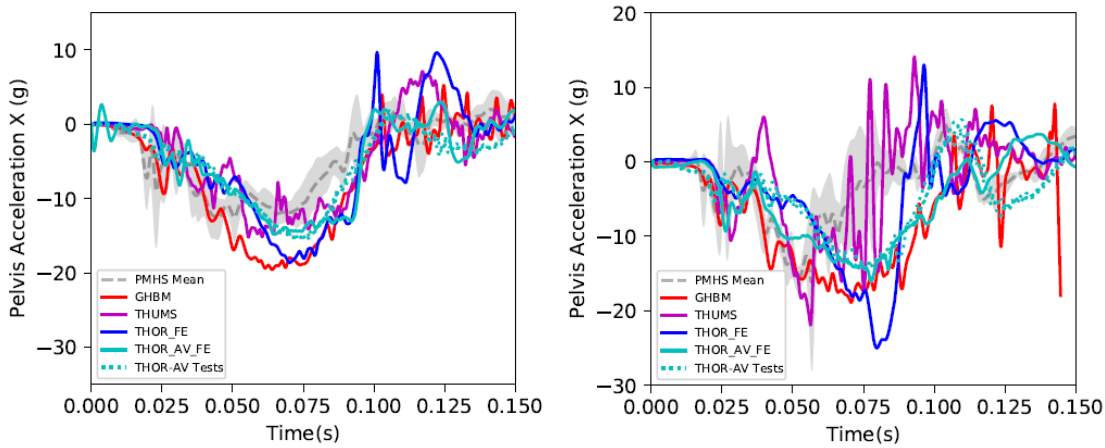


Figure A39. Pelvis acceleration X in 25° (Case #3, left) and 45° (Case #4, right) seatback UMTRI test configurations

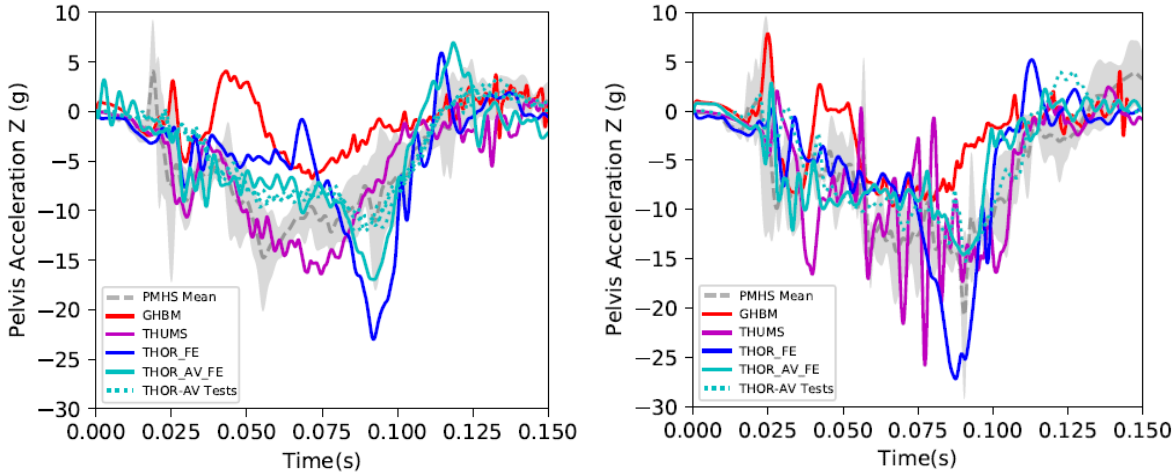


Figure A40. Pelvis acceleration Z in 25° (Case #3, left) and 45° (Case #4, right) seatback UMTRI test configurations.

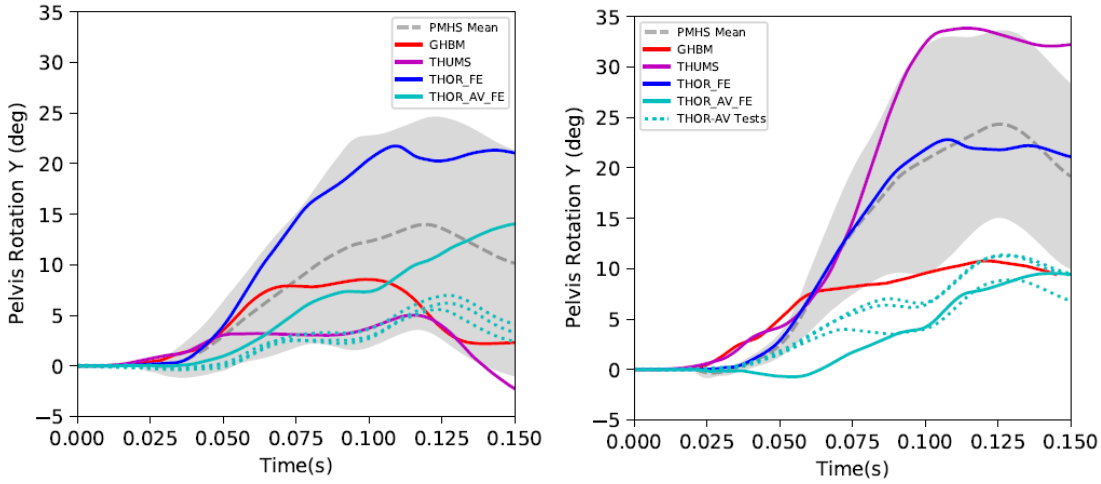


Figure A41. Pelvis rotation Y in 25° (Case #3, left) and 45° (Case #4, right) seatback UMTRI test configurations.

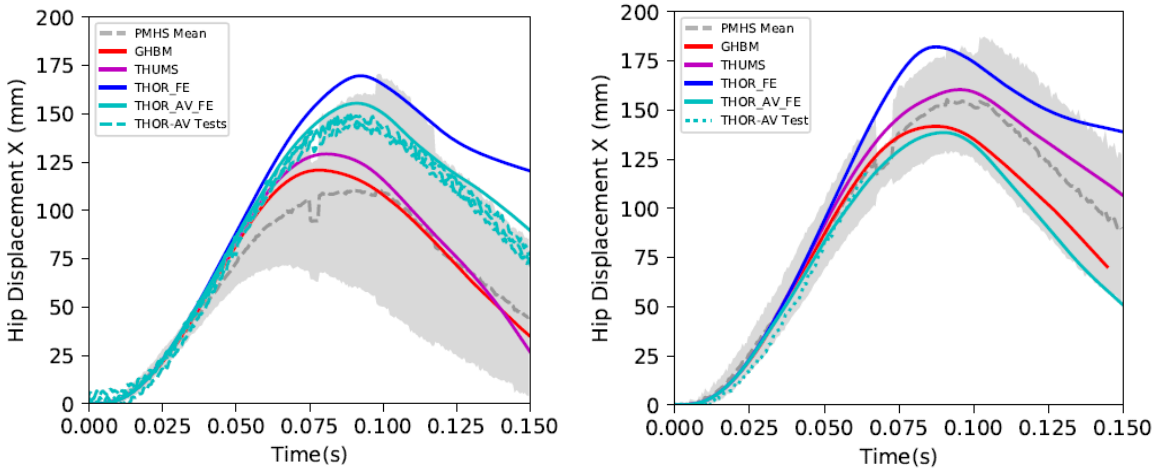


Figure A42. Hip displacement X in 25° (Case #3, left) and 45° (Case #4, right, partial data only in THOR-AV test due to the video target mounting bracket breakage) seatback UMTRI test configurations.

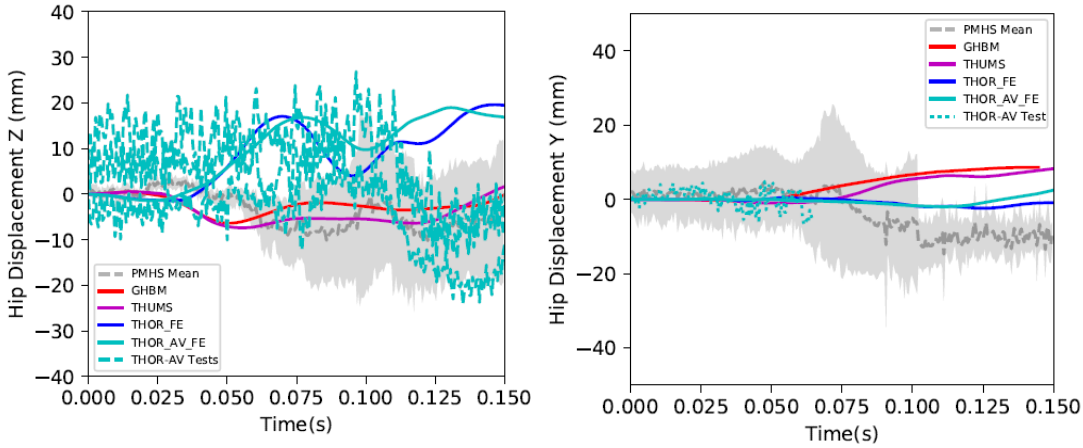


Figure A43. Hip displacement Z in 25° (Case #3, left) and 45° (Case #4, right, partial data only in THOR-AV test due to the video target mounting bracket breakage) seatback UMTRI test configurations